Geophysical Prospecting EAGE EUROPEAN ASSOCIATION OF GEOSCIENTISTS & ENGINEERS

Geophysical Prospecting, 2013, **61** (**Suppl. 1**), 505–532 doi: 10.1111/j.1365-2478.2012.01117.x

Review paper: Instrumentation for marine magnetotelluric and controlled source electromagnetic sounding

Steven Constable*

Scripps Institution of Oceanography, La Jolla, California, USA

Received July 2011, revision accepted June 2012

ABSTRACT

We review and describe the electromagnetic transmitters and receivers used to carry out magnetotelluric and controlled source soundings in the marine environment. Academic studies using marine electromagnetic methods started in the 1970s but during the last decade these methods have been used extensively by the offshore hydrocarbon exploration industry. The principal sensors (magnetometers and non-polarizing electrodes) are similar to those used on land but magnetotelluric field strengths are not only much smaller on the deep sea-floor but also fall off more rapidly with increasing frequency. As a result, magnetotelluric signals approach the noise floor of electric field and induction coil sensors (0.1 nV/m and 0.1 pT) at around 1 Hz in typical continental shelf environments. Fluxgate magnetometers have higher noise than induction coils at periods shorter than 500 s but can still be used to collect sea-floor magnetotelluric data down to 40–100 s. Controlled source transmitters using electric dipoles can be towed continuously through the seawater or on the sea-bed, achieving output currents of 1000 A or more, limited by the conductivity of seawater and the power that can be transmitted down the cables used to tow the devices behind a ship. The maximum source-receiver separation achieved in controlled source soundings depends on both the transmitter dipole moment and on the receiver noise floor and is typically around 10 km in continental shelf exploration environments. The position of both receivers and transmitters needs to be navigated using either long baseline or short baseline acoustic ranging, while sea-floor receivers need additional measurements of orientations from compasses and tiltmeters. All equipment has to be packaged to accommodate the high pressure (up to 40 MPa) and corrosive properties of seawater. Usually receiver instruments are self-contained, battery powered and have highly accurate clocks for timekeeping, even when towed on the sea-floor or in the water column behind a transmitter.

Key words: Magnetometers, Magnetotelluric, Electromagnetic.

1 INTRODUCTION

On land, it is fairly routine to employ electrical and electromagnetic (EM) methods to probe geological structure, using electrical conductivity as a proxy for porosity and rock type. Electrical methods include DC resistivity, induced polarization and self-potential measurements, which are used primarily for shallow groundwater studies and mineral exploration. Electromagnetic methods are distinguished by the use of inductive frequencies and are represented by the magnetotelluric (MT) and controlled-source electromagnetic (CSEM) methods. The MT method exploits the natural variations in the Earth's magnetic field that induce electric currents and fields

*E-mail: sconstable@ucsd.edu

in the ground. A frequency dependent transfer function between electric and magnetic fields is computed at some period range between 0.001–100 000 s, and is, in some sense, proportional to the electrical conductivity structure. The depth of investigation is determined by frequency and MT sounding can be used for shallow mineral exploration to deep mantle investigations. Controlled-source methods use a man-made source field to excite induced currents, using either magnetic coils or grounded electric wires. Measurements are made of the induced electric and/or magnetic fields as a function of source-receiver geometry and frequency (or transient decay for time-domain methods).

The extension of these geophysical methods to the deep sea-floor has always been challenging from the point of view of building and operating the necessary instruments. The first sea-floor measurements using the MT method were carried out in the 1960s by Jean Filloux and colleagues. Filloux used torsion fibre magnetometers (Filloux 1967) and a 'water chopper' electric field recorder using valves and salt bridges to reverse the connections to electrodes and thus remove electrode drift and self-potential (Filloux 1974; see also Filloux 1987). Although this approach continued to be used for several decades, the difficult mechanical engineering involved motivated other groups to utilize more conventional sensors. In the 1970s fluxgate magnetometers were incorporated into sea-floor instruments (Law 1978; White 1979) and are still in common use today. Poehls and Von Herzen (1976) used a thin-film magnetometer developed by Burroughs Corporation (Irons and Schwee 1972 provide a review of this sensor technology) in a sea-floor instrument. However, during the 1970s and 1980s it was still thought that water choppers were necessary to make low-frequency electric field measurements for MT soundings, although no other group had succeeded in replicating Filloux's technology. Poehls and Von Herzen (1976) circumvented the need to collect electric field data by using the vertical gradient of the horizontal magnetic field as a proxy for the electric field, combining sea-floor magnetic field measurements with those collected at nearby land sites. This vertical gradient approach has been used until relatively recently (e.g., Law and Greehouse 1981; Heinson *et al.* 1993; Jegen and Edwards 1998; Joseph *et al.* 2000).

The University of Tokyo group appears to be the first to start collecting data without the use of water choppers: Segawa and Toh (1992) made self-potential measurements in 1989 using a submarine to deploy a 40 m antenna with silver chloride electrodes and provided two electric field instruments for the 1988 EMRIDGE MT project (Heinson *et al.* 1993). Toh, Goto and Hamano (1998) described an instrument using silver chloride electrodes on 5.1 m dipoles with both fluxgates for MT sounding and nuclear precession magnetometers for observatory measurements. The group at Flinders University of South Australia developed integrated MT instruments consisting of fluxgate magnetometers and directly coupled electric field sensors, deploying them on the Reykjanes Ridge in 1993 (Heinson, Constable and White 2000) and the South Pacific MELT experiment in 1996/97 (Evans *et al.* 1999). Around that same time a collaboration started between Flinders University and Scripps Institution of Oceanography (California), using Flinders fluxgate magnetometers mounted on Scripps CSEM receivers equipped with DC-coupled electric field sensors. In this way long period sea-floor MT measurements could be made, first on the 1993 Reykjanes Ridge experiment (Heinson *et al.* 2000), on Axial Seamount in 1994 (Heinson, Constable and White 1996; Constable *et al.* 1997) and finally off Hawaii in 1997 (Constable and Heinson 2004).

As discussed below, the conductive ocean severely attenuates sea-floor magnetic fields at short periods and although fluxgate sensors have recently been used to collect MT data down to about 40 s (Heinson *et al.* 2000; Worzewski *et al.* 2011), all early MT data were limited to short periods of several hundred seconds at best. Sensitivity to a shallow structure is thus severely limited, exacerbated by the low conductivity of the oceanic lower crust and upper mantle, which serves to attenuate the magnetic field signals further. This led Cox (1980) to propose a CSEM method suitable for the deep sea-floor, using electric field transmitter and receiver equipment described in Cox, Deaton and Pistek (1981).

The high-frequency energy lost to MT is replaced by towing an EM transmitter close to the sea-floor (Fig. 1), which allows EM energy to couple with sea-floor rocks and propagate laterally to sea-floor receivers. The frequency of operation is typically 1–10 Hz for the original target of deep oceanic lithosphere structure but this has been expanded to about 0.1–30 Hz for exploration applications. The data consist of EM amplitudes and phases as a function of source-receiver offset, position and frequency. The more resistive the rock, the slower the amplitude decay with offset and the faster the apparent phase velocity and so CSEM measurements are preferentially sensitive to resistive material.

Sinha *et al.* (1990) developed a similar system, initially at Cambridge University, England and later at the University of Southampton. The U.K. and Scripps groups went on to use the CSEM method to study the geology of the oceanic lower crust/upper mantle (Cox *et al.* 1986; Constable and Cox 1996) and mid-ocean ridge systems (e.g., Evans *et al.* 1991; Sinha *et al.* 1996), often collaborating on projects.

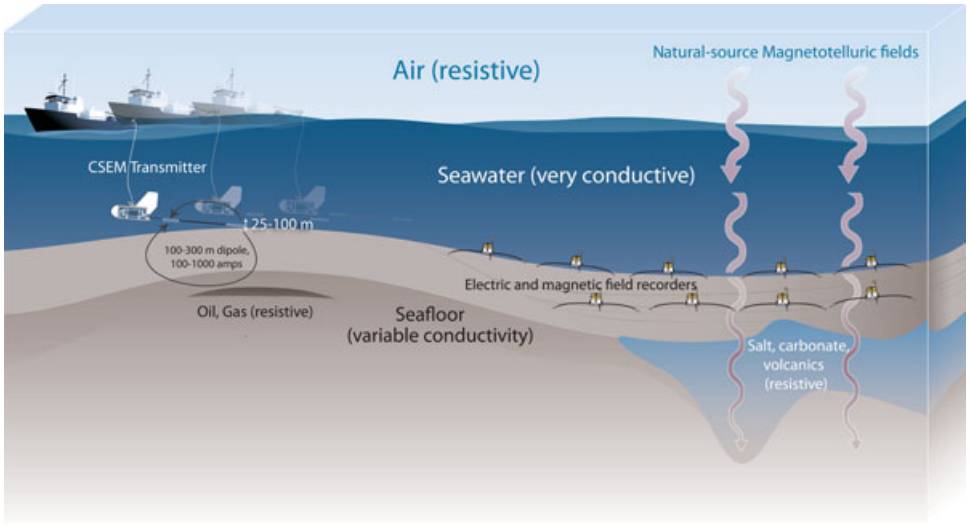

Figure 1 Marine MT and CSEM concepts, illustrated. For marine MT studies, sea-floor recorders make time series measurements of the Earth's varying magnetic field and the induced electric field, which can be interpreted to infer a deep geological structure. The addition of a CSEM transmitter, towed close to the sea-floor, allows these same instruments to map a shallow structure, including thin, resistive features such as hydrocarbon reservoirs.

Both the Scripps and Southampton groups used electric field transmitters and receivers. Magnetic transmitters and receivers can and have, been used for relatively shallow soundings but for deep soundings it is much easier to generate a large transmitter dipole moment using electric currents passed through the seawater than by using magnetic fields generated by loops or coils. Magnetic sensors were initially neglected on CSEM receivers because noise caused by motion in Earth's main field meant that they were much noisier than electric field sensors, which could make measurements to larger source-receiver offsets. Also, compared to electric fields, magnetic CSEM fields are relatively small over the more resistive geological environments typical of the early deep-water studies.

Interest in marine EM methods has grown considerably in recent years as a result of the commercial application of marine MT and CSEM sounding to offshore hydrocarbon exploration. The marine CSEM equipment developed for this study of the deep ocean floor could be applied to continental shelf exploration largely without modification. Equipment for continental shelf MT exploration, on the other hand, had to be explicitly developed for this application in order to extend the performance to periods short enough to be sensitive to the upper few kilometres. An early attempt at adapting land equipment to shallow marine exploration by Hoehn and Warner (1983) demonstrated the concept but was too cumbersome and too noisy for commercial application. Modification of marine CSEM receivers by Constable *et al.* (1998) for use as 'broadband' continental shelf MT recorders successfully extended the range of MT measurements down to 1–10 s by using induction coil sensors along with large concrete anchors to improve instrument stability.

Because electric current is preferentially induced in conductive material, the MT method is primarily sensitive to conductors and one classic exploration application of MT is the detection of sediments below resistive volcanics or carbonates. However, if the geological units are large compared with the depth of burial then the geometry of resistive features can be mapped and the early development of marine MT for hydrocarbon exploration was motivated by the need to map base of salt in the Gulf of Mexico (e.g., Hoversten, Constable and Morrison 2000; Key, Constable and Weiss 2006). Since depth of penetration can easily reach mid-mantle depths, from an exploration point of view there is no practical depth limitation to the MT method.

The intrinsic sensitivity of MT sounding to conductive rocks and the largely horizontal induced current flow, make MT practically useless for detecting thin, sub-horizontal resistive targets such as oil and gas reservoirs. However, CSEM is sensitive to such structures through increased lateral propagation associated with larger skin depths in resistive layers, combined with a galvanic interruption of vertical currents generated by the electric dipole transmitter. This is especially so in deep water, where CSEM measurements may be made without the confounding effects of EM propagation in the (resistive) atmosphere. In shallower water, energy propagating up to the

atmosphere and back down to the receivers (often called the air wave) becomes significant but sensitivity to the target structure may still remain, or even be enhanced in cases where the air wave interacts constructively with the target (Orange, Key and Constable 2009). The application of EM methods to commercial exploration owes much to instrumentation developed by the academic groups described above. The first proof-of-concept marine CSEM surveys for oil exploration, supported by Statoil (Ellingsrud *et al.* 2002) and ExxonMobil (Constable and Srnka 2007), relied on Scripps and Southampton University for all the EM equipment that was used and several commercial operators offering marine EM services today are using equipment based largely on these academic designs. Although the exploration industry adopted the electric dipole-dipole geometry, the low-noise magnetic sensors developed for broadband MT measurements coupled with the larger magnetic CSEM fields over conductive, continental shelf sediments has meant that modern magnetic recorders can operate at ranges similar to the electric receivers. Indeed, conversations with contractors suggests that some early commercial CSEM receivers collected better magnetic field data than electric field data.

Given the recent interest in marine EM methods it seems timely to review the design and use of instrumentation for marine EM data collection. To a large extent, everyone who tackles the formidable problem of building EM equipment for operation in the marine environment has to deal with the same set of problems and challenges, which this paper attempts to present in a general way. However, while an extensive review of the literature has been attempted, academic groups tend to report equipment parenthetically to the scientific results obtained by the data collection, often without going into detail about the instrumentation. Commercial groups tend not to publish and even actively avoid disclosing how equipment is constructed and operated, for a variety of reasons. As a consequence, when it comes to specific details of instrument design and construction this paper has to draw mainly on the author's own experience and equipment. However, in many respects the Scripps equipment described here is representative of the techniques and components used by others and it is hoped that the opportunity to present some of the details of the design will prove useful and interesting to the reader.

2 ELECTRO MAGNETIC FIELDS AND THE MARINE ENVIRONMENT

Before we consider the design of marine EM instrument systems, it is useful to examine the environment in which we work and the signals we wish to measure, since the characteristics of the ocean environment have a considerable impact on many aspects of instrument development and construction.

2.1 Field magnitudes

Figure 2 shows approximate amplitude spectra for magnetotelluric fields on the sea-floor of the continental shelves (represented by 1 Ωm sediments in 1 km water) and deep ocean basins (4 km water overlying 1000 Ωm sea-floor), along with sensor noise for magnetometers and electric field sensors (based on a similar figure by Key 2003). Sea-surface magnetic fields are approximated by the global spectrum of Constable and Constable (2004) and downward continued using field ratios for layered media given in Constable *et al.* (1998). While magnetic fields observed on land are one or two orders of magnitude above the sensor noise across the entire spectrum, this is not true on the sea-floor. Inductive attenuation of the higher frequencies in seawater effectively removes the signal above 0.1–10 Hz, depending on water depth. Over the resistive sea-floor, magnetic field attenuation extends to periods as long as 10 000 s or more. One way to explain this is that the magnetotelluric impedance, proportional to the ratio of horizontal electric and magnetic fields, must increase on or near the sea-floor and since the electric field must be continuous, the magnetic field must decrease. This is discussed further in Key (2003) and Constable *et al.* (1998). The depressed magnetic fields, and induced electric fields as low as 10^{-9} V/m/$\sqrt{\text{Hz}}$, place considerable demands on instrumentation for marine MT acquisition in the period range of 1–100 s, the very periods at which the MT method is sensitive to the structures of interest in continental shelf exploration.

For CSEM surveying, the peak sensitivity to the canonical oilfield model discussed by Constable and Weiss (2005) occurs at a source-receiver range of 6 km, where the electric fields have decayed to about 10^{-14} V/Am^2 and the magnetic fields to about 10^{-17} T/Am. Even with a large transmitter dipole moment of, say, 100 kAm, this requires noise floors before stacking of around 10^{-9} V/m/$\sqrt{\text{Hz}}$ and 10^{-12} T/$\sqrt{\text{Hz}}$ for even a modest signal-to-noise ratio of 10. While this again places demands on instrumentation, the CSEM signals are above the MT noise except at the lowest frequencies in shallower water.

2.2 Temperature

Temperature of seawater below the thermocline is very stable and is close to 3° C in deep water (1 km and deeper) except in

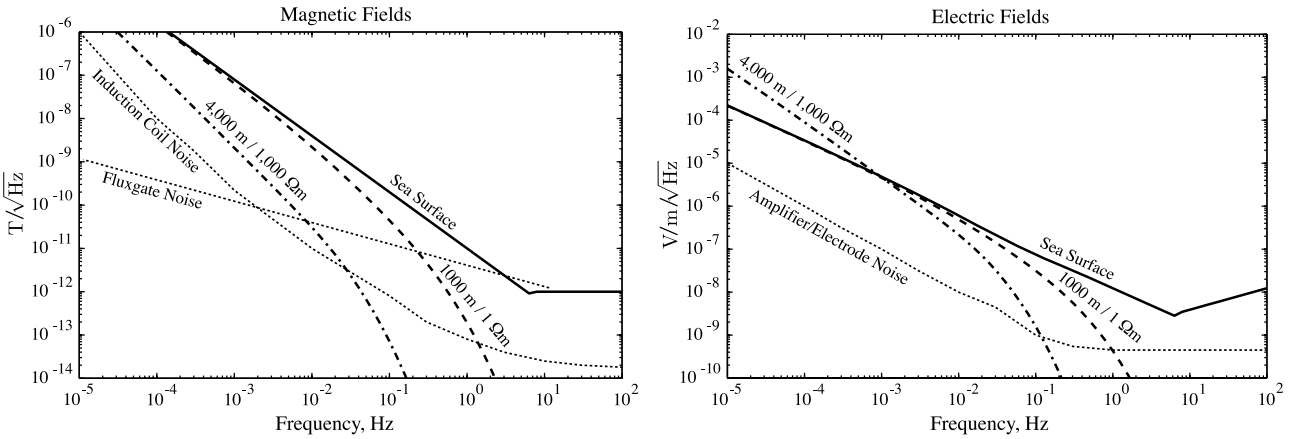

Figure 2 Magnetic fields at the sea-surface and downward continued 1 km to the sedimented sea-floor on the continental shelf and 4 km to the volcanic sea-floor in the deep ocean, along with the corresponding induced electric fields (sea-surface electric fields are for the continental shelf model). Noise floors are shown for a BF-4 induction coil magnetometer from EMI, Inc., a low-noise ring-core fluxgate based on data from Ripka (1992) and the electric field instrument noise shown in Fig. 6.

arctic and sub-arctic regions, where it can get as low as −2° C. The stability of the temperature in deep water, with temporal variations of less than 0.1 K, is an advantage; all instruments and sensors are sensitive to temperature to some extent and on land it is sometimes difficult to mitigate the impact of temperature changes that can exceed 40 K in a single day. For example, the electrodes used in land MT have to be buried quite deeply if long period measurements are required.

On the other hand, although stable, the relatively cold sea-floor temperatures can produce some problems. Until recently, disk and tape drives were used in instruments to store data and most of these were only rated for a temperature range of 5–50° C. Many would indeed fail on the cold sea-floor, particularly since they were turned on only when needed (to save power) after sitting cold for some time. The solution was to test various brands to find those that worked better than the specification, which several did. This problem has largely disappeared with the use of solid state mass storage but other problems, such as that of condensation, remain. Since instrumentation may be assembled on a vessel in a humid, sometimes quite hot, environment, significant condensation can occur inside the instrument on deployment in cold water, creating problems with electronics. The solution is to use a desiccant inside the instrument and to replace humid air trapped inside the pressure case with either ambient air passed through desiccant or inert dry gas (e.g., nitrogen) from compressed gas bottles. Another effect of the low temperature is that battery capacity (discussed below) is reduced over the specifications given for operation at 20° C.

2.3 Electrical conductivity of seawater

Water is electrically very conductive, with a resistivity around 0.3 Ωm, depending on salinity and temperature. Except for the Mediterranean and regions exposed to river outflow, salinity is almost constant at around 35g/l dissolved solids but water shallower than about 1 km and particularly above the thermocline can have highly variable temperature from around freezing to as much as 30° C or more. A commonly used linear relationship between seawater conductivity σ_w and temperature T (in Celsius) of Becker *et al.* (1982)

$$\sigma_w = 3.0 + 0.1T \quad \text{S/m} \tag{1}$$

is accurate to 3–5%. A cubic relationship of Perkin and Walker (1972) is more accurate over the 0–25° C range, which Constable, Key and Lewis (2009) modified slightly to improve high temperature (100–200° C) extrapolation:

$$\sigma_w = 2.903916(1 + 0.0297175T + 0.00015551T^2 - 0.00000067T^3) \quad \text{S/m}. \tag{2}$$

It can be seen from either of these relationships that seawater conductivity can vary by almost a factor of two between the surface and the sea-floor. Figure 3 shows a profile of temperature and inferred conductivity from an expendable bathy-thermograph (XBT) taken in the eastern Pacific.

The high conductivity of seawater means that the input impedance of electric field amplifiers need not be as high as on land. Similarly, the antenna impedance of electric transmitters can be made very low to reduce the power requirements,

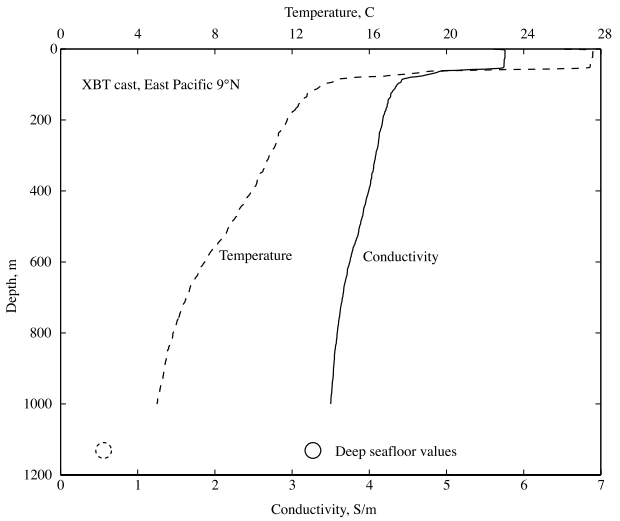

Figure 3 Temperature and inferred conductivity for the upper 1 km from an expendable bathy-thermograph in the eastern Pacific Ocean.

while still providing considerable currents. However, it is also becoming clear that marine CSEM studies need to include measurements of the seawater conductivity profile, as the data contain a significant signature associated with the water conductivity, even that close to the sea-surface (Orange *et al.* 2009; Key 2009; Constable *et al.* 2009). Seawater conductivity can be estimated from XBT temperature data but a direct measurement can also be made if a conductivity-temperature-depth (CTD) sensor is mounted on the transmitter. Alternatively, dedicated CTD casts can be made in the survey area.

2.4 Motion of water and instrument sensors

Water currents generate a variety of noise sources for sea-floor EM measurements. The most obvious one is the physical shaking of the instrument, which is particularly troublesome for magnetic field measurements. Any changes in the orientation of a vector magnetometer will change the size of Earth's magnetic field B_E that is coupled to the sensor:

$$B_{sensor} = B_E \cos\phi \tag{3}$$

$$\frac{\partial B_{sensor}}{\partial \phi} = B_E \sin\phi, \tag{4}$$

where ϕ is the angle between the sensor and Earth's field. When the sensor is maximally coupled into Earth's $\approx$ 40 μT field, the noise floor of a good induction coil magnetometer ($\approx$ 0.05 pT) corresponds to a change in ϕ of about one nanoradian, or one millimetre in a thousand kilometres. Motional noise will be within an order of magnitude of this unless the sensor is aligned to within a few degrees of Earth's field (in which case the orthogonal sensor will be maximally coupled anyway).

The motion of electric field antenna wires at velocity **u** in Earth's magnetic field will result in induced electric fields:

$$\mathbf{E} = \mathbf{u} \times \mathbf{B}, \tag{5}$$

so a strumming on antenna cables of order 1 cm/s (e.g., a frequency of 1 Hz with an amplitude of a few millimetres) will generate electric fields as large as 0.1 μV/m, well within the range of measurement.

Finally, the motion of seawater through Earth's field will induce an electric field of similar $\mathbf{E} = \mathbf{u} \times \mathbf{B}$ form and the resulting electric currents will generate a magnetic field. Cox, Filloux and Larsen (1971) estimated fields a large as 1 μV/m and 3 nT for baroclinic tidal currents on the continental shelves. The period of the tides (43 000 s) is far removed from CSEM periods (0.1–10 s) and greater even than most of the longest period MT signals measured, but variations in water flow and turbulence will generate higher frequency signals that are seen on both electric and magnetic sensors up to a frequency of several Hertz.

2.5 Sea-floor pressure

Pressures at sea-floor depths, even on the continental shelves, are high enough to make the engineering of waterproof cases, flotation and electrical connections a non-trivial business. The density ρ_w of seawater is 1028 kg/m^3, so pressure at h = 4 km depth is $\rho_w g h = 40$ MPa (5800 psi), where gravitational acceleration g is 9.8 m/s^2. The total force on a standard 43 cm (17 inch) diameter glass oceanographic float is 23 million Newtons with a stored energy of 1.7 Megajoules. During failure, the resulting implosion will usually destroy all the equipment in the vicinity.

2.6 Seawater corrosion

Seawater is a relatively corrosive fluid and almost all structural metals, except possibly titanium, will degrade after lengthy exposure. This is particularly true of the stronger aluminium alloys rich in zinc and magnesium, which can corrode across the entire thickness of a pressure case or end cap in a few weeks. Even the better grades of stainless steel will undergo cavity, or anoxic, corrosion over time. Corrosion creates a very noisy electrical environment and it is important that low-noise electric field sensors be isolated from metals and in particular dissimilar metals in contact with each other.

3 ELECTRIC FIELD MEASUREMENTS

In principle the measurement of an electric field in seawater is simple – make contact with the water using two electrodes and connect these to an amplifier using insulated leads. The output of the amplifier is recorded either onboard a ship (for cable systems) or using an autonomous logging system. For large signals resulting from short-offset CSEM or DC-resistivity measurements this simple approach is all that is needed and stainless steel electrodes and standard amplifier designs have been used to collect good data. However, for marine MT and long-offset CSEM studies such systems are orders of magnitude too noisy to be useful.

3.1 Marine electrodes

Electrodes form the interface between an ionic conductor (seawater) and the metallic conductor of the antenna leads. A good description of electrodes for marine use can be found in Corwin (1973). A small amount of current necessarily must be drawn in order to make a voltage measurement and any resulting charge flow into one electrode must be balanced by the flow out of the other electrode completing the circuit. The charge must be carried across the electrode interface in a reversible way, because if the charge is consumed in an irreversible electrochemical reaction on one electrode a galvanic potential or polarization will be generated, corrupting the measurement. For a simple bare metal electrode this reaction would be

$$\mathrm{M} \rightleftharpoons \mathrm{M}^{+} + e^{-}, \tag{6}$$

where M is the metal, M^{+} is the metal cation and e^{-} is an electron. This reaction is reversible if the ionic conductor contains a high concentration of M^{+}, which is exploited by the traditional copper-copper sulphate electrode used in land MT, whereby a copper rod is immersed in a saturated solution of copper sulphate and electrical contact with the soil is accomplished across a barrier of semi-permeable ceramic or similar material. However, for bare metal in seawater the concentration of metal ions is not high enough to prevent irreversible corrosion and associated noise and the dominant cation is sodium, which would make a most unsuitable electrode for other reasons. (Copper sulphate electrodes would prove problematic in the ocean because of the high chemical gradients across the semi-permeable interface.)

A modification of the bare metal electrode is to coat the surface of the metal with a relatively insoluble metal salt and immerse this in a solution of the compatible anion. Both the lead-lead chloride electrodes used on land and the silver-silver chloride electrodes used in marine EM work fall into this category. For the latter, a silver wire, rod, or plate is coated with silver chloride and immersed in a solution of potassium chloride or, for marine use, sodium chloride. The reversible reaction becomes

$$\mathrm{Ag} + \mathrm{Cl}^{-} \rightleftharpoons \mathrm{AgCl} + e^{-}. \tag{7}$$

The relative insolubility of silver chloride and its compatibility with the major anion in seawater makes this a stable and practical electrode for marine use. It is desirable to isolate the electrode surface from seawater both physically and chemically, which is often done by packing silver chloride around an electrode surface inside a porous container. The silver chloride ensures that the water surrounding the electrode surface is saturated in silver ions. The silver chloride coating can be achieved either by sintering and baking or by electro-plating. The key to producing electrodes with low self-potential differences and low susceptibility to common mode changes in temperature and salinity is clean and uniform construction. There is also some evidence that increasing the size of the electrode or electrode surface lowers noise and in any case one will want to maintain a contact resistance with seawater of less than the Johnson noise of the desired sensitivity. Because of the high conductivity of seawater, a much lower contact impedance can be achieved (a few Ohms) than on land (hundreds of Ohms at best, usually a few kΩ). Johnson, or thermal, noise power is given by

$$V_J^2 = 4kTR, \tag{8}$$

where k is Boltzmann's constant (1.4×10^{-23} J/K), T is absolute temperature and R is resistance. In order to maintain a noise level below 1 nV, noise resistance has to be kept below about 200 Ω. This precludes the use of very small electrodes and also salt bridges, in which the electrode is mounted close to the instrument and the antenna is formed from a plastic pipe flooded with seawater (e.g., Filloux 1987).

The construction of marine silver-silver chloride electrodes is described in Webb *et al.* (1985) and Filloux (1987). An example is shown in Fig. 4. A strip of pure silver foil is wrapped around a plastic rod and soldered to an underwater connector in the electrode end cap, with the joint back-filled with epoxy to prevent access of seawater to any non-silver metals. The silver is cleaned with 30% aqueous nitric acid solution and rinsed with de-ionized water. A porous plastic tube is cemented or press-fit to the end cap and the void packed with a mixture of silver chloride and an inert silica filler. A second cap is glued on to contain the packing and the entire

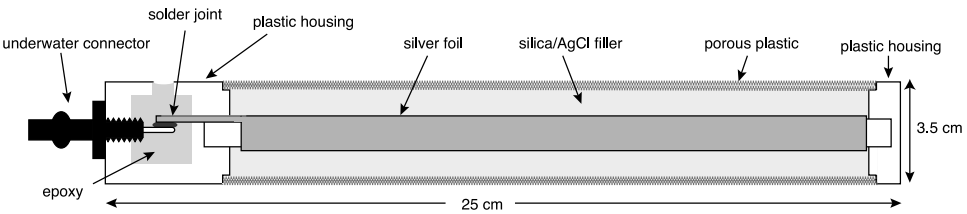

Figure 4 A marine silver-silver chloride electrode, as described in Webb *et al.* (1985) and in extensive current use for marine CSEM and MT measurements.

electrode immersed in a solution of 35 g/l reagent grade sodium chloride. The electrode is thoroughly wetted with this solution by cycling between a vacuum and atmospheric pressure. The surface of the silver is then plated with silver chloride by anodizing using a constant current of 1 A for 120 s. After storage of about one week the DC potential between the electrodes is below 0.01 mV. With use this will rise to about 0.1 mV and electrodes are rejected if the self-potential rises significantly above this. The silver chloride in the packing helps to maintain the plating on the surface of the silver but presumably during use the electrode is contaminated with anions and cations other than silver, chlorine and sodium. The resistance of such a pair of electrodes in seawater is about 6 Ω at 10 Hz.

The Ag-AgCl electrode is probably unsurpassed for marine EM measurements but the need to keep the electrode wet is seen as a disadvantage by some and has encouraged the use of other types, such as carbon fibre electrodes (Crona *et al.* 2001). These, and other dry electrodes, are polarizable, or capacitive and so do not perform as well as Ag-AgCl at low frequencies, but in practice the lower frequency MT signals may be large enough that an adequate signal-to-noise ratio is maintained. Indeed, capacitive coupling is often used to remove self-potential from MT and CSEM measurements and so capacitive electrodes may be a viable option. However, little data have been published on their performance in the 1000 s period range.

3.2 Amplifiers

Voltage differences across the electrodes are very small and need substantial amplification before digitization and recording. The frequencies of operation, even at the higher end of marine CSEM acquisition (10 Hz or more), are low by the standards of amplifiers and so the ubiquitous $1/f$ noise associated with semiconductors becomes an issue that must be addressed. The standard approach to this is the use of 'chopper' amplifiers, in which the incoming signal is modulated (chopped) at a relatively high frequency, amplified at a favourable part of the $1/f$ spectrum and then de-modulated to restore the low-frequency signal. Alternatives to the chopper amplifier for low-frequency, low-noise applications are few and usually involve relatively high-power consumption, such as the parallel transistor design described in the Analog Devices SSM-2210 application note, which achieves a $\sqrt{N}$ noise reduction by using N components, at a power cost of 2 mA per component.

Figure 5 shows a modern version of the marine EM amplifier described by Webb *et al.* (1985), which consumes only 1 mA per channel from a ±5–7 V supply. A notable aspect of this amplifier is the use of transformer coupling immediately after the MOSFET bridge that does the chopping. The transformer performs a combination of isolation and buffering and provides a small amount of gain. Isolation is important. Electric field amplifiers for broadband land MT have traditionally exploited optical isolation amplifiers to ensure that no resistive connection between grounded electrodes and instrument 'ground' occurs. More modern high-input impedance amplifiers and analogue-to-digital converters (ADC) have allowed the direct connection to differential amplifiers. It is, however, hard to make a high-impedance amplifier without significant resistance and component noise, which is typically measured in the $\mu V/\sqrt{Hz}$ range. This is acceptable on land with signals of order mV/km and electric field dipoles of order 100 m, but well above what is required for marine EM. The appropriate approach to marine measurements is to take advantage of the low impedance of the electrode-seawater system by having a relatively low-input impedance to the amplifier. However, a low-resistance connection between the electrodes and the 'ground' of the amplifier, ADC and logging electronics (much of which is digital and relatively noisy) is likely to create noise on the input signal. It is also a poor idea to connect instrument ground to a metal pressure case, since corrosion potentials can put significant noise into the amplifier.

Figure 6 shows a noise spectrum of such an amplifier with a shorted input, collected on the seafloor in 900 m of water. The data as collected (A) are flat and around 2 $nV/\sqrt{Hz}$, although after the instrument response is applied (B) we see

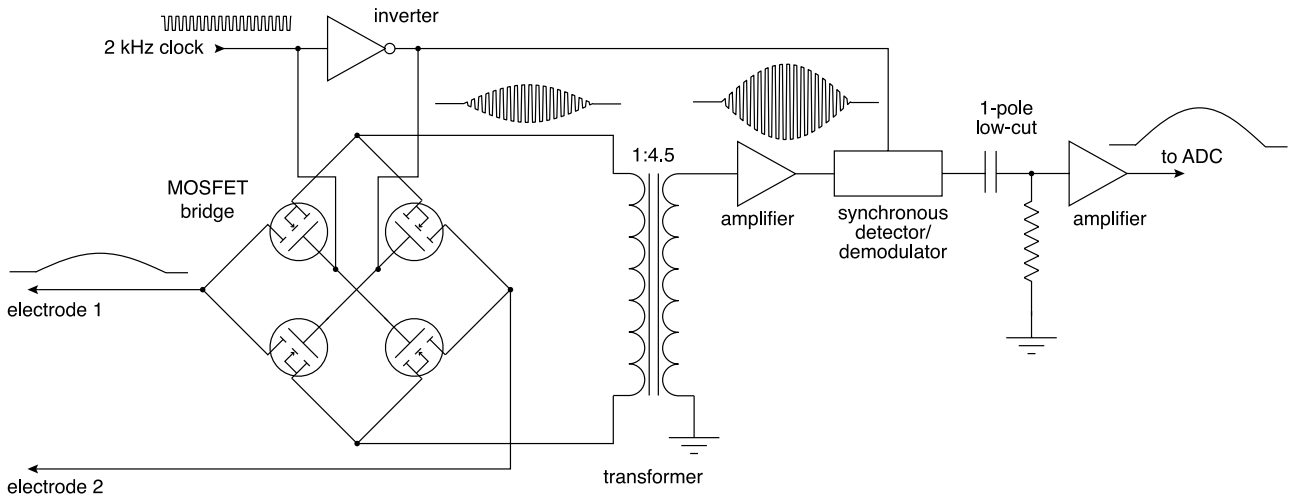

Figure 5 The Deaton electric field chopper amplifier, described originally in Webb *et al.* (1985), which uses a MOSFET bridge to reverse the incoming signal at 2 kHz and a transformer to perform a combination of isolation and buffering, as well as provide a small amount of gain.

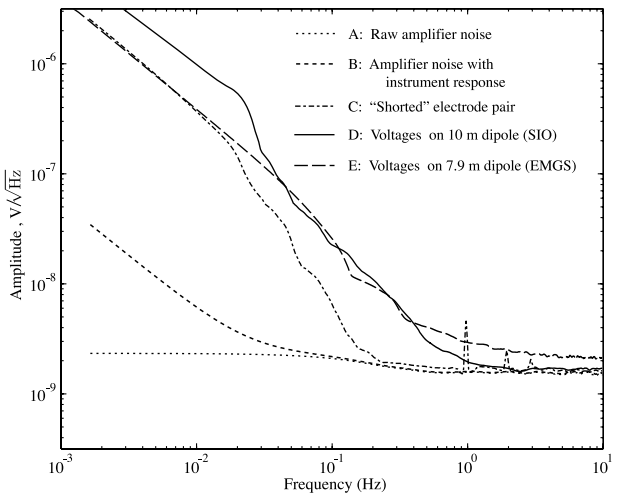

Figure 6 Voltage amplitude spectrum obtained by shorting the amplifier input during a receiver deployment in 900 m water off Australia, both as measured (A) and with the instrument response included (B). Spectrum (C) was obtained by mounting electrodes adjacent to each other on the receiver frame (the signals at 1 Hz and harmonics are from the instrument time base (clock), which occasionally appears in some instrument channels). For comparison MT voltages recorded on deepwater deployments of a Scripps instrument (D) and an EMGS instrument (E) are also shown.

an effective increase in low-frequency noise associated with the low-cut filter. The amplifier noise floor is equivalent to a Johnson noise on a 250 Ω resistor. Two electrodes were also mounted adjacent to each other on the receiver instrument (C), exhibiting white noise above 0.2 Hz, which is attributed to the chopper amplifier described above. The red $1/f^2$ spectrum below 0.2 Hz is characteristic and probably associated with the electrodes, although some MT noise may be leaking through. Typical magnetotelluric signals recorded on a Scripps receiver (D, 900 m water depth) and an industry instrument (E, 2.5 km depth) are also shown. Magnetotelluric signals meet the instrument noise floor at around 1 Hz.

Since amplifier and electrode noise are both voltage, rather than electric field sources, it seems fairly obvious that an improved signal-to-noise ratio for electric field measurements can be achieved through the use of longer antennas. Indeed, the main subject of Webb *et al.* (1985) was the use of 'LEM' instruments having a single, long antenna. These instruments have proved very effective in deep water, with antennas up to 3 km long having been deployed (Constable and Cox 1996), and with the expected improvement in the signal-to-noise ratio being achieved. We can convert the noise floor power P_n in Fig. 6 to a noise floor E_n for receiver dipoles of length L, over a stacking window t_s seconds long using

$$E_n = \frac{\sqrt{P_n}}{L\sqrt{t_s}} \quad . \tag{9}$$

For 10 m dipole receivers and 1 minute stacks this is about 2×10^{-11} V/m (to obtain CSEM noise we divide by the source dipole moment; for example, with a 100 kAm transmitter and 1 minute stacks the noise floor is about 2×10^{-16} V/Am^2). On continental shelves we do not always see the expected improvement from the use of LEM instruments, nor the expected noise floor on the standard receiver instruments. In an example shown in Fig. 7, both a standard receiver with 10 m antennas and a LEM with 100 m antennas were deployed near each other in 900 m water on the North-west Shelf of

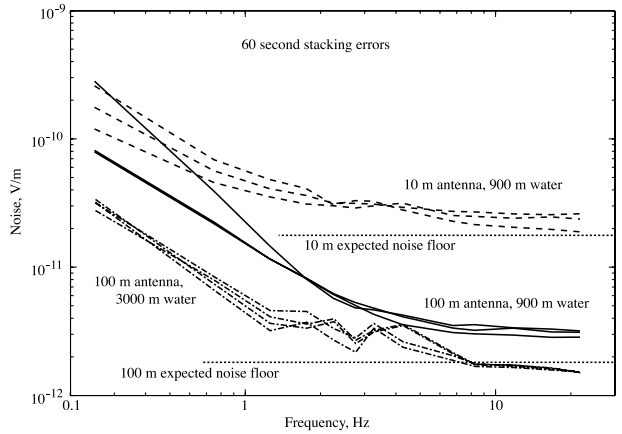

Figure 7 CSEM noise for three examples of a standard receiver instrument with 10 m electrode arms and LEM instruments with a 100 m antenna, deployed in 900 m water off Australia and in 3 km water off Nicaragua. Noise estimates were obtained from the stacking variance of 60 s stack frames (Myer, Constable and Key 2011). Dotted lines are expected noise floors computed from the amplifier and electrode noise shown in Fig. 6.

Australia. At the lowest frequencies the noise is similar for the two antenna lengths and well above the expected noise floor. This suggests that an environmental source of electric fields is the limiting factor for this particular time, place and frequency, which we suspect in this case is probably caused by water currents. At 2 Hz and above, the standard instrument is close to the expected noise floor and the LEM, while not achieving the expected factor of 10 improvement, is much quieter than the 10 m instruments. Again, this suggests that the LEM is still measuring environmental noise even at the higher frequencies. If one compares this to a LEM deployed in the deep ocean, in this case 3 km water off Nicaragua, one sees that the expected noise floor is finally achieved at the highest frequencies (around 10 Hz).

4 MAGNETIC FIELD MEASUREMENTS

For both MT and CSEM measurements, a vector field magnetometer is required, negating the use of total field nuclear resonance sensors such as proton precession and alkali vapour instruments. Fluxgates and induction coils are the two sensors in main use today. Although not immediately apparent, both are applications of Faraday's Law for a coil consisting in N turns of wire around the core of permeable material with cross-sectional area A, generating a potential difference V from a time varying magnetic flux dB/dt:

$$V = -NA\frac{dB}{dt} = -NA\mu_e\mu_o\frac{dH}{dt}. \tag{10}$$

An induction coil relies on time variations in magnetic field H. The permeable core provides an effective increase in flux through the coil by a factor of μ_e, which for a long cylindrical coil of high permeability with a length divided by diameter of a is approximately

$$\mu_e = \frac{a^2}{\ln(2a) - 1} \tag{11}$$

(Tumanski 2007). The relative permeability of mu-metal alloys after annealing in a reducing atmosphere is of order 10^5 and for a coil of order 1 m long and 1 cm diameter μ_e is about 10^4. Because μ_e is limited by the core geometry, rather than the permeability of the material, the effect of temperature on the permeability of the core can largely be ignored.

We see that V increases with frequency and coils have a characteristic one-pole response across the frequency band of operation. This represents a good match to the MT source field spectrum (see Fig. 2), although high-cut filtering in the amplifier is often used to flatten the response at high frequencies. Large N is achieved by making the windings out of very fine wire and the dominant source of noise becomes the thermal resistance noise, or Johnson noise, of the wire. Here we see the second advantage of a long, thin magnetometer. Piling windings upon windings increases the diameter of the turns and so resistance starts to increase more rapidly than V (because the flux is largely captured by the core material). Indeed, since the majority of the magnetic flux is only captured near the centre of the core's length, it is preferable in terms of signal-to-noise ratio to limit the windings to the central 2/3 of the core. If the only two considerations are Johnson noise and the output voltage, it is easy to show that the signal-to-noise ratio V^2/V_J^2 is simply proportional to the total volume of windings, or, equivalently, the weight of the coil, regardless of the N resulting from the wire gauge chosen. For this reason aluminium wire can be used where weight is an issue (often the case for marine coils), since although the resistance is 55% higher, the weight is only 30% that of copper. Also, to keep the density of the windings as high as possible, the wire can be passed through a mandrel to make it rectangular in cross-section, attaining a 27% decrease in resistance per unit volume. One still needs a low-noise amplifier with a gain of order 10 000 to produce useful signals from an induction coil and the usual trade-offs between power and noise arise.

A good induction coil magnetometer has a noise level of about 0.1 pT/$\sqrt{\text{Hz}}$ at around 1 Hz, with a red noise spectrum at lower frequencies because of the dB/dt loss of sensitivity. The high-frequency response is limited by inductive losses in the core material and capacitance of the windings. The latter

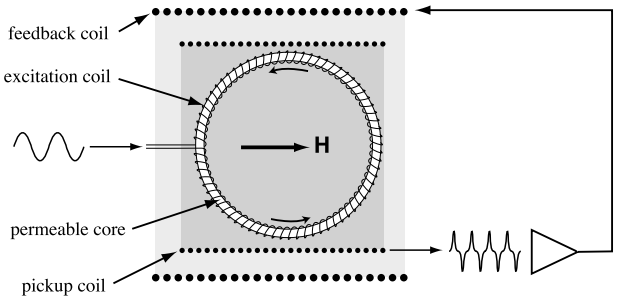

Figure 8 Principles of operation for a ring-core fluxgate magnetometer. An excitation current saturates the core sooner on the side aligned with the external field and later on the opposite side. This induces a voltage in the pickup coil at twice the excitation frequency, which may be used as a feed-back signal for a nulling coil. Feedback and pickup coils can be combined.

is mitigated by winding the coils on discrete bobbins, rather than along the length of the core. The former can be reduced by laminating the core material or using a ceramic for the core.

Fluxgates generate a time varying flux for a nominally static magnetic field by creating a time varying effective permeability:

$$V = -NA\frac{dB}{dt} = -NA\mu_o\frac{d\mu_e}{dt}H \quad . \tag{12}$$

This is accomplished by saturating the core with an excitation coil, since a saturated core has an effective permeability of zero, creating a variable μ_e. Excitation frequency is typically around 1 kHz. Various core geometries can be used but sensors with the lowest noise tend to be ring-cores (Fig. 8). The excitation coil saturates the two sides of the core in opposite directions, saturating earlier in the side parallel to the magnetic field and later in the side that is anti-parallel. The asymmetry generates a net flux at twice the excitation frequency, which is detected using a pickup coil and fed to a lock-in amplifier operating at twice the excitation frequency. If the output is rectified and used to control a feedback coil, the field can be nulled and the current in the feedback coil becomes the magnetic field measurement. Operating instruments as null sensors generally improves linearity and reduces temperature effects. The unsaturated μ_e for a ring-core is approximately the diameter divided by the thickness, which are typically 2 cm and 1 mm.

A high-quality ring-core fluxgate magnetometer has a noise of about 4 pT/$\sqrt{\text{Hz}}$ at about 1 Hz with a $1/f$ power spectrum associated with Barkhausen noise (sudden, discretized changes in magnetic domain orientation) in the core material (Ripka 1992). Figure 2 provides a comparison of fluxgate and induction coil noise referenced to sea-floor and sea-surface fields, showing that the noise for the two sensors crosses at about the 500 s period. Fluxgates can collect sea-floor MT data beyond this towards shorter periods but run into loss of signal at periods of 10–100 s. Induction coils extend this short period response by nearly a decade, particularly over continental shelf sediments. One can collect induction coil MT data to about 1 Hz in 900 m water depth during times of good magnetic activity but 5–10 s is a more typical short period limit.

Induction coil noise remains below sea-floor MT signals to long periods and one can reliably collect 10 000 s MT data on instruments deployed for several weeks. The near-constant temperature of the sea-floor environment probably improves the long period performance of induction coils over their use on land. Although fluxgates clearly have a signal to-noise-ratio advantage at long periods, deployment times of several months are required to extend the long period limit much beyond 10 000 s no matter what sensor is used, and only occasionally are MT data to 100 000 s reported for sea-floor sites.

Since most marine CSEM surveying is carried out in the 0.1–10 Hz frequency range, induction coils are the optimal CSEM sensor, although fluxgates can be used if smaller signal-to-noise ratios can be tolerated. It is important to note that the excitation circuits of a fluxgate sensor can be extremely noisy, easily corrupting low-noise electric field CSEM data collected on the same instrument.

5 DEPLOYED INSTRUMENT DESIGN

Although there are currently several groups working on a variety of cable and towed marine EM systems, which exploits the fact that continuous electrical contact can be made with seawater even when being towed through the medium (see Section 7), at this time most marine MT and CSEM operations depend on free vehicle deployments, in which an instrument is sunk to the ocean floor using some sort of anchor, makes autonomous measurements and is then released from the anchor by acoustic command to return to the surface by virtue of self-buoyancy. The need to be buoyant immediately places a premium on the instrument being light and, because batteries are one of the heavier parts of the system, low in power consumption.

5.1 Housings and flotation

While it is possible to make spherical metal instrument cases that are self-buoyant, most groups use added buoyancy to

instrument packages. The two flotation options are oceanographic borosilicate glass spheres and syntactic foam. Glass spheres are commercially available in sizes up to 43 cm (17 inch) diameter, providing a net lift of up to 25 kg with an effective density of about 0.4 times seawater. Besides being efficient in terms of buoyancy, this kind of flotation is relatively inexpensive. On the negative side, the packaging and mounting of spheres is not always volumetrically efficient, they need to be handled with a modicum of respect and they do, occasionally, fail. The failure rate is low; over a career of about 5000 sphere-deployments, the author has had only one confirmed implosion of a glass ball. However, other groups have reported higher loss rates for spheres deployed repeatedly in deep water. Between the combination of flotation loss and implosive force, the consequence of a failed glass sphere is always the loss of an instrument.

Syntactic foam is a related product made from casting small, hollow glass microspheres 10–200 μm in diameter in a plastic resin. The advantages of syntactic foam are that it is robust to handling, will never fail catastrophically and it can be cast into arbitrary shapes. The density for material rated to full ocean depth is about 0.55 times seawater. The downsides are the greater expense over glass spheres and the greater air-weight per unit buoyancy.

Glass floats can be used as pressure cases to house instrument electronics. Spheres designed for this purpose are formed as two matched, split hemispheres with precision ground surfaces that are aligned and dry-mated without grease or glue. The outer edge is sealed with rubber vulcanizing tape. The advantages of this approach are that the instrument package is easily made self-buoyant, is inexpensive and not subject to corrosion. The disadvantages are that electrical feed-throughs are more difficult to make and are less reliable than those for metal cases and that opening and closing the case to change batteries, retrieve data, etc., is a delicate operation in which the edges of the ground surfaces are easily chipped, making the housing useless. For any application where the instrument need never be opened, glass housings can be a good choice, especially when glass buoyancy is being used anyway.

The three main choices of metals for instrument pressure cases are various alloys of aluminium, titanium and stainless steel. The strengths of these materials are somewhat similar but the weight in water approximately doubles as one goes down this list, starting with 1.7 kg per litre for aluminium (see Table 1).

The strength-to-weight ratio of aluminium alloys with high zinc and magnesium content makes them attractive for seafloor instrument housings, which need to form self-buoyant structures. (Unfortunately, this makes these materials also ideal for nuclear isotope centrifuges and the 7075-T6 alloy is a restricted export material when formed into tubes greater than 75 mm in diameter.) These alloys are highly corrodible and are usually anodized (electrically coated with a layer of aluminium oxide about 0.04 mm thick) to protect the surface. Anodizing is, by its nature, a slightly porous structure and so it is advisable to paint exposed surfaces, or use liberal quantities of grease on the (necessarily) unpainted surfaces used for O-ring seals. It is also important to avoid contact with dissimilar metals of any kind and use only plastic or rubber materials for mountings. If constructed and maintained in this way, such instrument housings will last indefinitely.

Table 1 Materials for instrument housings, yield strength (compressive strength is used for glass) and density in air (ρ) and seawater (both normalized by seawater density ρ_s).

Material	yield strength MPa	yield strength kpsi	air density ρ/ρ_s	submerged density $(\rho - \rho_s)/\rho_s$
Aluminium 7075-T6	506	73	2.7	1.7
Titanium Alloys	700–1,400	100–200	4.5	3.5
Stainless Steel 316	240	35	7.9	6.9
Borosilicate glass	290	43	2.3	1.3

The corrosion resistance of both titanium and stainless steel is far superior to aluminium and were it not for the cost, titanium would be the natural choice in terms of strength-to-weight ratio but for cost reasons stainless steel is often used when durability and corrosion resistance are required, with a trade-off of substantially increased weight.

For the 7075-T6 aluminium alloy, a ratio of 1:8 wall thickness to radius will support ocean pressures to 6 km depth for arbitrarily long cylindrical pressure cases. Such cases weigh about the same as the water they displace and so do not contribute to the weight of an instrument in water (and thus can be made long without penalty). The end caps, however, are much thicker and amount to dead weight that must be offset by flotation. The wall thickness can be made somewhat smaller if the case is machined accurately cylindrical and kept round by supporting end caps or stiffening rings every two diameters along the length (Brown and Cox 1973). Hemispherical or spherical cases can be made with even thinner walls and can have substantial self-buoyancy.

Plastics make good materials for instrument frames because they are light, resistant to seawater and, particularly in the case of aluminium pressure cases, will not contribute to the

electrolytic corrosion associated with dissimilar metals in contact. Fibreglass and PVC are strong but heavier than seawater. Polypropylene is very tough and the lightest of plastics but is not particularly easy to machine. Polyethylene is also lighter than seawater and presents a good compromise in machinability, buoyancy and strength.

5.2 Release mechanisms

The standard approach to oceanographic free vehicle deployment is to use acoustically triggered release mechanisms. An acoustic transponder system, usually the same unit being used for navigation (see below), activates a release mechanism after hearing a coded signal sent from the survey/research vessel. The scientific research community has tried all manner of release systems for sea-floor instruments (including dissolving sugar and electrolytically corroding magnesium) but two types of acoustic release are available commercially. The first, designed specifically for moorings, uses a latching mechanical system that is integrated into the pressure case. These are well suited to in-line loads but tend to jam and fail for sea-floor instruments, in which side-loading is possible. The second type uses a mechanism often called a 'burn wire', in which a small length of stainless steel or a similar inert, strong metal holds together the latch of a mechanical lever. When a release signal is detected, a positive voltage of order 10 V with respect to seawater is applied to the wire, which then electrolyses away in a few minutes. With an appropriately designed mechanical system, burn wires are very reliable and easy to actuate, since they simply require a latching electrical switch, such as a silicon controlled rectifier (SCR). They also have the advantage that they can be tested immediately prior to deployment without actually triggering the mechanism, by connecting a load between the burn wire and the seawater ground pin and measuring the voltage or current. Disconnecting the load should reset the release. The load should be such that the current drawn is comparable to that of the burn wire in seawater, usually of order 1 A.

5.3 Logging systems

Availability of modern digital electronics makes the digitization and storage of data streams easier than ever before but autonomous sea-floor recording still presents some special challenges. One reason for this is that most commercial logging systems for use on land tend to fall into two categories, neither of which is particularly useful for sea-floor recorders. One category is represented by high-end systems designed to operate at fast data rates with a lot of flexibility, where data collection is carried out directly onto a laptop or desktop computer that controls the digitization electronics. Even geophysical equipment designed for field use on land usually has such a computer with a standard operating system integrated into the hardware. These systems tend to be too large, too power hungry and too dependent on real-time interaction with an operator to be useful on the sea-floor.

The second type of commercially available logging systems are small, battery powered units designed for autonomous logging of a low-data rate and low-dynamic range environmental parameters such as, for example, temperature. These systems tend not to be sophisticated enough for marine EM work. Although the very first version of the instrument described by Constable *et al.* (1998) was based on a high-end system of this type, it required the addition of memory, an external clock, interface circuitry and a disk drive. It was quickly replaced by custom electronics.

A second reason to avoid commercial loggers is that the power consumption of even the autonomous commercial units, and certainly that of the more capable systems, is too high for use in small pressure cases that need to be floated to the surface. The largest part of the payload of a marine EM data logging system, measured either in weight or volume, is likely to be the batteries. Since an extra kilogram of batteries is likely to require an extra half to one kilogram of pressure case material, both of which will need to be floated by adding about twice that weight in buoyancy material, a kilogram of batteries costs up to six kilograms of total instrument air weight.

The third problem with off-the-shelf loggers is that in an autonomous sea-floor instrument, the logging electronics have to be located within a few tens of centimetres of the amplifiers and magnetic field sensors. Any fluctuation in power consumption will create huge signals (i.e., noise) on the data channels. In one example (from actual experience), if the real-time software is allowed to increase the CPU clock speed for a few milliseconds every few seconds in order to move data between memory buffers, this can be enough to put a near-saturating spike in magnetic field data. These issues are rarely addressed during the development of commercial logging systems.

Another concern rarely addressed adequately by commercial data loggers is the need to keep accurate time. Data collected by simultaneously recording sea-floor instruments need to be merged based on time of collection. While the global positioning system (GPS) has revolutionized the ability to tell time accurate to a few microseconds anywhere on the planet's

surface, GPS signals are not, of course, available beneath the conducting ocean. Autonomous sea-floor instruments must have onboard clocks to keep time, although GPS provides a convenient way to set instrument clocks before deployment and measure drift on recovery. Timekeeping again presents trade-offs between power and accuracy. Quartz crystal oscillators need to be kept at a constant temperature to have a constant frequency and so crystals for accurate clocks are held in thermostatically controlled ovens at a temperature above ambient, around 50–60° C. This represents too much power for sea-floor instruments. A practical alternative is to calibrate the temperature response of the crystal and to use a microcomputer to measure temperature and correct for the crystal frequency using a calibration table. In this way oscillators stable to a few parts in 10^9 consuming only one or two milliamps can be made, accurate to a few milliseconds per day. This is barely adequate – if phase accuracy of one degree at a frequency of 1 Hz (either CSEM or MT) is required, time must be accurate to about 3 ms over the period of deployment. Advances in low-power micro-fabricated atomic clocks (e.g., Knappe *et al.* 2005) suggest that an alternative to quartz oscillators will be available sometime in the future.

Figure 9 shows a block diagram of a typical logging system. Data are formatted by a central processing unit (CPU), time stamped and stored in a temporary RAM buffer in order to minimize the increased noise and power consumption associated with the mass storage device (true even for solid state memory cards). When the RAM buffer fills (usually every few hours or more, depending on sample rate) the mass storage device is turned on and the data are moved to non-volatile storage, an activity that may put a brief burst of noise into the data (assuming that the CPU 'double buffers' the data in order to continue sampling during data transfer).

5.4 Batteries

Batteries quickly become a critical issue for marine free vehicles because they are a significant part of the weight budget and failure can mean loss of a data set or even an instrument. Considerations are power, weight, cost and reliability and there are various trade offs, the foremost of which is single-use versus rechargeable. Single-use batteries tend to be reliable and energy-efficient at the cost of continuous replacement and opening instruments for installation. Rechargeable batteries are cost-effective and allow sealed pressure case operation but eventually cause loss of data when they are mistakenly deployed uncharged, or reach the end of their life span. The various chemistries currently available are described below and summarized in Table 2.

Lithium single use batteries have the highest energy density available, with a D or DD cell providing 450–510 Watt-hours per kilogram (Wh/kg), making them the battery of choice for long deployment oceanographic instrumentation. They have a very low-internal impedance, so low that they are usually internally fused to prevent fire or explosion in the case of accidental shorting (their energy density is a little less than half that of the explosive TNT). The very flat discharge curve means that full voltage is maintained until near the end of the battery's life but also means that the remaining capacity cannot be gauged by measuring voltage under load. These batteries also 'passivate'; after partial use followed by storage, the electrode surfaces become contaminated and the output

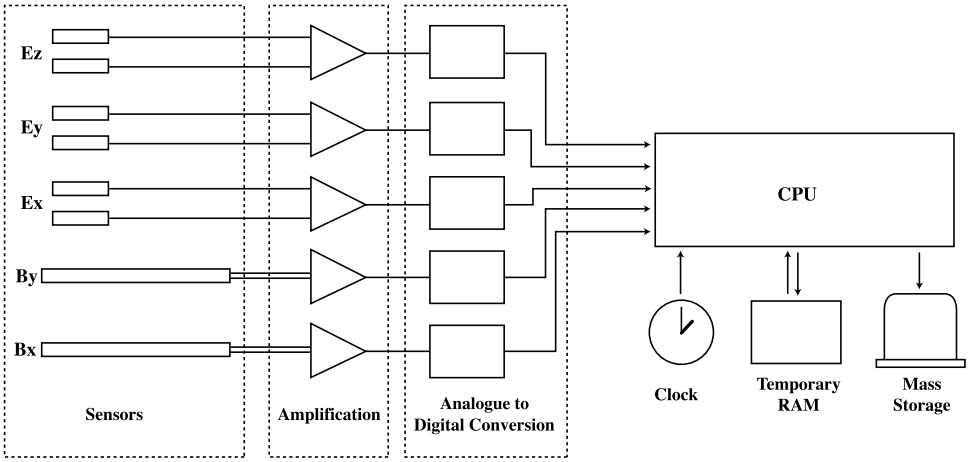

Figure 9 Block diagram of a logging system for sea-floor EM field recording. Sensor signals are amplified, digitized and collected by a central processing unit. Data are time stamped and kept in a RAM buffer until the buffer is full, at which point in time the mass storage device is switched on and data in the RAM buffer stored on non-volatile media.

Table 2 Capacities of batteries. See text for further discussion of the various battery types.

Chemistry	Wh/kg	notes
Lithium single use	450–510	best capacity, expensive, hazmat issues
Alkaline single use	150	economical and safe, large voltage drop
Nickel Cadmium	40	obsolete
Nickel-metal hydride	80	good capacity, tolerant of full discharge
Lead-acid	30	poor capacity, intolerant of full discharge
Lithium-ion rechargeable	200	good capacity, management of charge/discharge required

voltage decreases and internal impedance increases, an effect that may be reversed by loading the cell and drawing significant current, during which the voltage will increase over the period of a few minutes to near full voltage. The cells are expensive (of order US$100 per DD cell at the time of writing) and are potentially hazardous to use since they can vent toxic fumes, ignite, or even explode if mis-handled or placed in contact with seawater. They must be handled and shipped as hazardous material and cannot be flown on passenger aircraft. Lithium fires require the use of specialized extinguishers.

Single use alkaline cells are inexpensive, reliable, easy to obtain, safe to use and have a fairly good capacity (150 Wh/kg for a D cell). Their biggest disadvantage is that they have a fairly high internal impedance and need to be drawn down from 1.5 V/cell to a voltage of 0.8 V/cell to obtain full capacity, often requiring the use of voltage converters, which can either create noise or consume power.

Nickel cadmium batteries have a low-internal impedance (a D cell is rated to deliver over 200 A), a flat discharge curve and are moderately tolerant of full discharge, which eventually happens during sea-floor deployments. At a measly 40 Wh/kg for a D cell they have been largely superseded by the more modern NiMH cells.

Nickel-metal hydride (NiMH) cells have similar advantages to the older Ni-Cad cells (low impedance, flat discharge, good capacity, tolerant of full discharge) with a better energy density (80 Wh/kg for a 'fat-A'). One significant problem is self-discharge, whereby the cell loses capacity at about 5% per month, precluding use for long deployments and requiring charging before use, although some versions advertising low self-discharge are becoming available.

Lead-acid cells have a low-output impedance and a fairly flat discharge curve and are inexpensive. They have the advantage of being tolerant to continuous trickle charging, making them useful as a backup battery system but are extremely inefficient (30 Wh/kg for a D cell) and intolerant of full discharge. Large car-type lead-acid batteries can be pressure compensated in an oil bath and operated at full ocean pressure when weight is not a problem and one wishes to avoid pressure cases.

Lithium-ion rechargeable batteries, used commercially for cell phones and laptop computers, are now becoming available as discrete cells with good capacity (200 Wh/kg for a D cell), low impedance, flat discharge and low self-discharge. The main problem is that they require a complicated management of the charge/discharge cycle and are somewhat hazardous, since the cells can catch fire if overcharged or fully discharged.

5.5 Receiver orientation and position

Since autonomous EM receivers free-fall to the ocean floor, one needs a means to record their position and orientation. Surface and other currents will result in instruments drifting from the point where they are released from the survey vessel – about 100 m drift in 1 km water would be typical. This uncertainty may be tolerable for MT work, certainly for regional studies, but is not at all tolerable for CSEM sounding. Orange *et al.* (2009) showed that to obtain CSEM data accurate to 1%, one needed positions accurate to 5 m and orientations accurate to 8°. The only solution for navigating the deployed locations of receivers is to install acoustic transponders on the receivers and to range on them from the vessel after deployment. Two basic types of acoustic systems are in use.

Long base line (LBL) acoustic systems rely on triangulating a target location using ranges obtained from several widely spaced transmitter or transponder positions. In this case the survey vessel ranges on the sea-floor receiver from at least three locations (in practice it would range repeatedly while driving some pattern over the deployed position). Frequencies are around 12 kHz, which has been long established as a good compromise between resolution and ability to transmit acoustic energy long distances through water. Although the wavelength is about 10 cm, in order to obtain some frequency resolution and discrimination bursts (pings) of sound about 5 ms long are used. Two-way traveltime is 750 m/s and traveltime discrimination is usually accurate to about 1 ms, providing about a metre of resolution for a single ping. Inverting a sensible survey pattern (two crossing lines or similar over the instrument) using a measured water velocity profile

and curved raypaths provides instrument positions accurate to a few metres. The equipment for this type of navigation is simple, requiring a 12 kHz transducer on the vessel along with GPS position, and capable of working up to ranges of 10 km and water depths of 6 km.

Short baseline (SBL, also super short-baseline or SSBL and ultra-short baseline or USBL) acoustic systems use higher operating frequencies than LBL acoustics. Measurements of phase differences over an array of receiver transducers are made to obtain the angle of incoming acoustic energy as well as the traveltime. The ranging system is mounted on the vessel and consists in several transducers spaced as widely apart as possible (SBL) or a large array of transducers mounted on a single assembly (SSBL and USBL). The pitch, roll and heading of the vessel need to be monitored continuously using a motion reference unit (MRU) in order to convert the incoming angle to a vector in space. Such systems are able to operate at ranges up to 3 km with advertised accuracies of about 0.25% in range and about 0.25° in angle. Thus, under ideal operating conditions, one might expect range errors of no worse than 8 m and cross-range errors of no worse than 13 m for a position estimated from a single vessel location. In practice these figures may be optimistic. Experience suggests that temporary installations of portable SSBL systems tend not to perform as well as permanently installed and calibrated systems. For sea-floor receiver navigation, an SBL system can be used in the same mode as an LBL system (by driving a pattern with the vessel) in order to obtain similar accuracies.

Some sort of recording magnetic compass, often incorporating a tilt sensor, needs to be mounted on the instrument to record orientation on the sea-floor. Isolating the compass measurement from magnetic components in the instrument, such as induction coil cores and batteries, can be difficult. Industry clearly has had problems with making accurate compass measurements and Mittet *et al.* (2007) described a way to recover receiver orientation from CSEM fields when the compass measurements fail or are too inaccurate. Weitemeyer (2008) described a different approach to the same problem but solving for the transmitter orientation as well, and Key and Lockwood (2010) described a scheme to recover receiver orientation during 1D inversion of CSEM data. Myer, Constable and Key (2012) made 134 comparisons of orientation derived from CSEM data and from an external recording compass and showed that the means agreed to within less than a degree and the standard deviation was about three degrees, which places an upper bound on the error from the recording compasses. Of course, receivers could be positioned using remotely operated vehicles (ROVs) and although this would be time consuming and expensive it may be necessary for repeat surveys carried out to observe changes in hydrocarbon reservoirs during production.

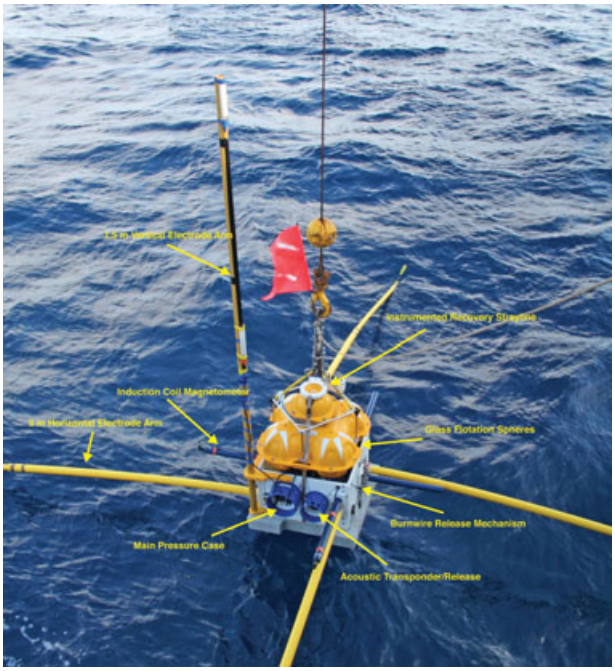

Figure 10 Scripps sea-floor EM recorder being deployed.

5.6 Scripps ocean-bottom electromagnetic receivers

An annotated photograph of the current Scripps ocean-bottom electromagnetic (OBEM) receiver is shown in Fig. 10. This is a third-generation (Mk III) design, first deployed offshore Angola in 2001 (Constable and Srnka 2007), with the electronics system housed in a 14.5 cm diameter cylindrical pressure case. It follows the second-generation (Mk II) instrument described by Constable *et al.* (1998), which was first used in 1995 offshore Sicily. The Mk II instruments use an 18 cm diameter pressure case but the internal electronics have been progressively upgraded to make them functionally equivalent to the Mk III design for the instruments still in use. The first generation instruments (Webb *et al.* 1985) started life in a 30.5 cm diameter pressure case but became smaller (20 cm) as the large tape drives in the older instruments were replaced with smaller tape drives and then disk drives (Constable and Cox 1996). The Mk I instruments were decommissioned after 2001.

The Mk II/III receiver assembly is approximately 1 m on each side, weighs about 100 kg in air and has electric field

dipoles of 10 m in the horizontal and 1.5 m in the vertical. The electric field noise on the horizontal components is 0.1 nV/m/$\sqrt{\text{Hz}}$ at 1 Hz and the magnetic field noise is about 0.1 pT/$\sqrt{\text{Hz}}$ at 1 Hz. Up to 8 channels of data can be digitized at 24 bit resolution at sample rates of up to 1000 Hz (maximum rate for multiple channels is 6000 Hz divided by the number of channels). With 4 channel sampling at 125 Hz (for example) the total power consumption (logger plus amplifiers) is 370 mW, providing a maximum duration of about 200 days with lithium primary cells for power or about 50 days on NiMH batteries, limited by the size of the main pressure case and the buoyancy budget. Data are stored on a compact flash card, which at the time of writing was available in capacities of up to 64 Gbyte (which would allow the 200-day deployment mentioned above). The total depth rating is 6 km, and when attached to a concrete anchor the instrument sinks at about 60 m/minute. The package is self-buoyant by about 15 kg and rises at 20 m/minute during recoveries. The long-term loss rate in normal working environments is less than 1%, averaged over about 1500 deployments and recoveries, using a custom-made acoustic release system.

The original Webb *et al.* (1985) amplifier, designed specifically for marine CSEM studies, had an input impedance of about 50 Ω. This has been increased to about 1 kΩ in the current design. A coupling capacitor was connected between the electrodes and amplifier in the original design to remove low-frequency MT noise and self-potentials from the CSEM signals and also prevent the input transformer from saturating on DC current. The coupling capacitor was retained in the Mk II broadband MT instrument (Constable *et al.* 1998) but the input impedance and capacitance were both increased to lower the corner frequency to around a 1000 s period and facilitate MT data collection. Later, improvements in electrode design (reducing self-potentials), smaller antenna lengths and a lower gain on the first stages of the amplifier all allowed the omission of the coupling capacitor in the Mk III instruments for both CSEM and MT applications. Retaining the higher input impedance mitigated the negative impact of having a connection between the electrodes, which allows a DC current to pass and potentially de-plate silver chloride from one of the electrode surfaces and/or saturate the input transformer.

It has been noted that movement of a magnetometer in the Earth's main field will create noise. To minimize motion on the sea-floor, the Scripps instrument uses a large 80 cm by 80 cm by 10 cm slab of concrete with an air weight of approximately 200 kg, to which the instrument is well coupled by two mechanical release mechanisms using burn wire actuators, both tightened to a torque of 5.6 Nm (50 inch-pounds) on a 3/8″-16 threaded rod. A single stainless steel strap connects the two mechanisms, passing through two stainless steel loops set into the anchors. If one release fails, the other release can be fired to recover the instrument. This system was developed specifically in order to collect low-noise MT measurements – electric field measurements are much more forgiving of anchor design. Non-magnetic materials are used throughout the anchor (and instrument frame) to avoid distortion of Earth's field and any noise associated with time-varying magnetic properties.

Voltages from sensors are amplified and passed to an analogue-to-digital converter (ADC). In the Mk I instrument, a 16-bit conversion was carried out through low-power voltage controlled oscillators whose output cycles were counted during the sample interval. In the early Mk II instrument, inputs from up to 4 channels were multiplexed into a very fast 16-bit successive approximation ADC. On the current Mk III instrument a delta-sigma 24-bit ADC is being used on each of up to 8 channels (and up to 4 channels on the upgraded Mk II instruments). The main advantage of 24-bit instruments is that the gain of the amplifiers can be lowered, increasing the dynamic range. However, comparison of data from the 16- and 24-bit instruments shows no difference in CSEM or MT data quality, largely because the noise floor is determined by the sensors and first stages of the amplifiers.

The first Mk II receivers used small computer systems interface (SCSI) disk drives for mass storage, which allowed rapid retrieval of data through the pressure case end cap data by bringing the 25 data lines required for this interface to a connector protected by a waterproof cover. The Mk III and upgraded Mk II instruments use compact flash cards for mass storage and an Ethernet interface through the end cap allows data recovery without opening the instrument but at a relatively slow rate. It is often more convenient to retrieve the data by removing the flash card when the batteries are recharged or exchanged.

To record instrument orientation on the sea-floor, Mk I Scripps receivers (Constable and Cox 1996) included simple small cameras that photographed a compass needle onto lithographic film, which was effective enough but hardly convenient for large numbers of instruments or deployments. The Mk II instrument described by Constable *et al.* (1998) used an external mechanical system that locked a compass needle after deployment, using dissolving sugar as a simple timed release to allow the instrument time to settle to the sea-floor. Any mechanical imperfections caused inaccuracies and while these worked well when newly made they became unreliable with use. The first Mk III sea-floor receivers used an electronic compass/tiltmeter mounted on the data logger inside

the main pressure case, which was powered and read by the logger whenever data were moved from RAM to mass storage. While convenient, this location was close to the internal batteries, which had to be de-gaussed to remove any remanent field in the cases, and also the induction coils, which distort the field considerably, and so large errors were possible. The current solution is to mount an autonomous compass-tiltmeter high on the instrument frame as far from the magnetic sensors as possible. This device is powered just before deployment and records orientation once an hour for the first 24 hours after deployment. It has proved reliable and is accurate to better than 3 degrees (Myer *et al.* 2012).

6 EM TRANSMITTERS

The purpose of a CSEM transmitter is to broadcast electromagnetic energy through the sea-floor at frequencies between about 0.05–50 Hz and in doing so provide the largest possible signal recorded at the receiver instruments. The electric and magnetic fields are proportional to the dipole moment of the transmitter, which for an electric dipole is given by the length L_a times the current I_a. For typical deep sounding transmitters dipole moments are of order 10^4–10^5 Am (industry transmitters output a thousand Amps or more on antennas 100–200 m long). For magnetic dipoles the moment is given by the number of turns in the coil, the current and the cross-sectional area of the coil.

Because of inductive attenuation in seawater, it is preferable to have the transmitter either on or close to the sea-floor to minimize losses and this also reduces the effect of the air wave. Having the antenna actually on the sea-floor, as was originally the case for the Scripps transmitter (Cox *et al.* 1986; Constable and Cox 1996) and is still the case for some shallow profiling systems (Yuan and Edwards 2000; Schwalenberg *et al.* 2010), reduces complexity, provides maximum coupling and removes one navigational parameter (i.e., height off the seabed). However, dragged transmitter systems cannot successfully be used in rocky environments or where significant seafloor infrastructure exists (i.e., well heads, pipelines, cables, etc.). In these cases it is preferable to 'deep-tow' the transmitter some distance off the sea-bed (typically 50–100 m). Deep-towed instrument systems were developed at Scripps in the early 1970s by Fred Spiess and colleagues (Spiess and Mudie 1970; Spiess and Tyce 1973) but pioneered for marine CSEM use by the Cambridge/Southampton group (the deep-towed active source instrument, or DASI, of Sinha *et al.* 1990).

To 'fly' the transmitter above the sea-floor requires that the antenna be approximately neutrally buoyant, which the Southampton group achieved by offsetting the weight of a copper antenna with an oil-filled streamer, an effective but bulky solution. The modern approach is to offset the weight of the conductor with low-density plastic, such as thermoplastic elastomer. Normally one would use copper for high-current conductors, since its conductivity of 0.59×10^8 S/m is second only to silver (which is only a few per cent better) but copper has a weight of 7.9 tonnes per cubic metre in water. Aluminium has about half the conductivity of copper, 0.38×10^8 S/m but has a submerged weight of only 1.7 tonnes per cubic metre and so for a given resistance is 1/3 the weight of copper, making it more practical to float using only plastic jackets.

Figure 11 shows the general approach used for CSEM transmitters. The ship's three-phase AC power is transformed up to high voltage for transmission to the underwater unit along the tow cable, where it is stepped down to low voltage and high current. The AC current is then rectified and switched to a low-frequency binary or ternary waveform for injection into the antenna. Variations and complications to this basic approach are discussed below. The design of a CSEM transmitter can be reduced to the effects of three input parameters; the resistance of the antenna to water, the total desired output current and the maximum voltage possible on the towing cable and other components. This then determines the turns ratios on the transformers, the required current carrying capacity of the tow cable and the total power required for the system.

6.1 Antenna resistance

Antenna resistance is a combination of cable resistance and grounding resistance of two electrodes. Cable resistance is simply given by the diameter, length and resistivity of the metallic conduction member. The resistance of the electrodes to seawater is mainly a function of seawater resistivity ρ_w and geometry; for a long cylindrical electrode the resistance per electrode is given by

$$R = \frac{\rho_w}{2\pi L_e}\left[\ln\left(\frac{2L_e}{a}\right) - 1\right], \tag{13}$$

(equation (3.09) of Sunde 1949) where L_e is electrode length and a is the diameter. Because a appears in the log term, the diameter has much less impact than length on grounding resistance. The current that can be obtained from a given voltage is essentially proportional to the electrode length but multiplying the diameter by 10-fold barely doubles the efficiency of the electrode (Fig. 12). This demonstrates clearly that

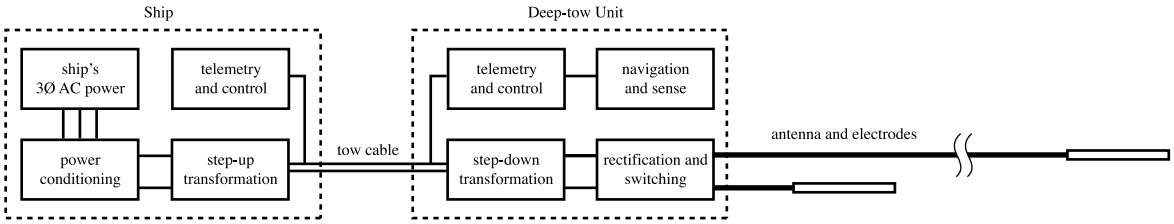

Figure 11 Block diagram of a CSEM transmitter system. The ship's power is conditioned (made into a variable voltage and perhaps converted to a higher frequency or single phase) and transformed to several thousand volts for transmission down the tow cable. In the underwater unit, the power is transformed to low voltage/high current, rectified and switched for output to the antenna. Bi-directional telemetry allows control of the underwater unit and monitoring of the navigation peripherals and environmental and current sensors.

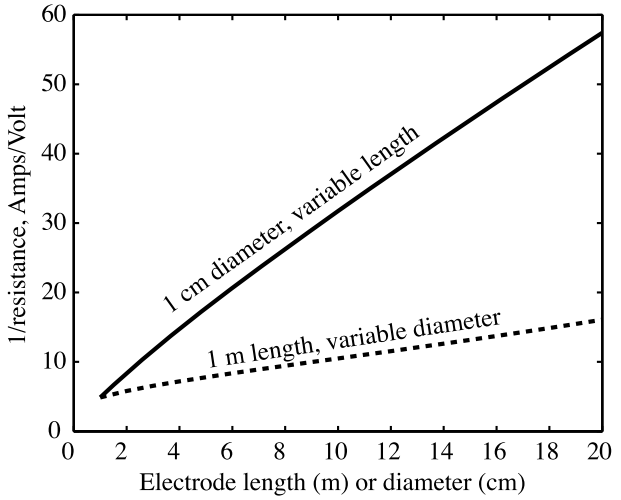

Figure 12 Effect of increasing a cylindrical electrode's length or diameter on its grounding resistance. Increasing the length of a 1 cm diameter electrode from 1 m to 10 m increases the current driven per volt from 5 A to 35 A. Increasing the diameter of a 1 m long electrode from 1 cm to 10 cm increases the current driven per volt from 5 A to only 10 A.

electrode grounding resistance is not simply a function of surface area, as one may mistakenly assume. Other geometries could be used, such as spheres, but long cylinders in the form of bare cable or pipe are logistically convenient. To lower grounding resistance by using electrodes in parallel one must separate the electrodes by a substantial fraction of their length, which is usually not convenient for towed marine applications.

The dipole moment of the antenna can be increased by increasing the length L_a and if the electrodes are kept at a constant fraction of the antenna length then the electrode resistance will decrease as L_a increases, even though cable resistance will increase. Thus for a given power and cable diameter, a longer cable will produce a larger dipole moment even if the output current is somewhat reduced. However, there are various reasons why antennas cannot be made arbitrarily long; there is the practical problem of towing a long antenna close to the sea-floor without actually having it touch the sea-bed, there is the complication of having to account for the antenna length in the analysis of the data (rather than use the dipole approximation for the bipole, which is generally good for ranges larger than about 3 antenna lengths) and ultimately there is the loss of resolution to lateral changes in resistivity. Typical antenna lengths vary between about 50 m used for hydrate mapping (e.g., Weitemeyer *et al.* 2006) and the 500 m used for the bottom-dragged antenna of the early Scripps systems (Cox *et al.* 1986; Constable and Cox 1996).

The logistical cost of increasing the dipole moment by increasing the current is much higher than increasing antenna length. Doubling the dipole moment by doubling the current requires four times the power dissipated in the seawater. The cost of transmitting this down the tow cable and the other losses in various components means that the total power required is almost double that delivered to the antenna, so a marginal increase in the signal-to-noise ratio comes at a substantial cost in transmitter power.

6.2 Antenna inductance and test loads

A CSEM antenna has an inductance as well as resistance, a result of the magnetic field generated by the current in the cable. As this magnetic field collapses during the switching of the current in the antenna the induced voltage must be accommodated by the transmitter circuitry. The self-inductance in μH of a long wire is given approximately by

$$Z = 0.2L\left[\ln\left(\frac{4L}{a}\right) - 0.75\right] \tag{14}$$

(Rosa 1908) and would typically be some hundreds of μH. This must be balanced by capacitance across the transmitter output to prevent voltage peaks from the back electromotive force (EMF) destroying the switching components.

The need to simulate both the resistance and inductance in the antenna for bench testing of transmitters, as well as dissipate tens of kilowatts, presents some interesting challenges for the construction of dummy loads. One solution is to wind air-cored solenoids using heavy-gauge insulated wire so that the total wire length provides the correct resistance and the solenoid provides the right inductance. Inductance in μH of an air-cored solenoid is given by Wheeler's formula:

$$L = \frac{N^2 D^2}{18D + 40L}, \tag{15}$$

where N is the number of turns, D is the diameter in inches and L is the length in inches (Wheeler 1928). Such coils can be water-cooled to dissipate power.

6.3 Power design considerations

Having chosen an antenna and computed its resistance, the remaining parameter is the tow cable operating voltage and power. For example, the standard 17 mm coaxial oceanographic cables supported by the Unified National Oceanographic Laboratory System (UNOLS) in the USA and elsewhere are rated to 3000 VDC (2100 Vrms). Higher voltages are possible for custom cables, although components rated higher than 2000 Vrms are expensive and of limited availability. A full ocean depth length (10 km) of this cable has a total resistance of 67 Ω and maximum power transfer will occur when the input impedance of the primary transformer of the transmitter equals the cable resistance, resulting in a cable current of 15 Arms at maximum voltage, or a maximum power rating about 30 kW. On shorter tow cables, up to 20 kW of this power budget can be delivered to the sea-floor unit but the additional losses in the transformers, rectifiers and switches limits the power available on the antenna to 17–18 kW. Various frequencies can be used to transmit power down the tow cable. Direct current (e.g., Evans 2007) is simple and provides most power for a given maximum voltage. Alternating current allows transformers to be used, either at conventional power frequencies (50/60 Hz, e.g., Constable and Cox 1996) or at higher, frequency stabilized frequencies. Sinha *et al.* (1990) used 256 Hz and the current Scripps transmitters use 400 Hz.

6.4 Waveform switching

The undersea unit must rectify AC power and then switch low-frequency binary or ternary transmissions to the electrodes. Several transmitter designs use a silicon controlled rectifier (SCR, also called a thyristor) bridge to accomplish both rectification and switching in one compact system. An important complication associated with this approach is that SCRs do not switch off until the current stops flowing. Because of the antenna inductance, the current is not in phase with the voltage by an unpredictable amount and so during switching one must monitor the current and wait to turn on the next pair of SCRs until the current drops to zero and the last pair turn off; otherwise all the SCRs will be on at once and there will be a short across the output of the transformer, which will cause it to fail. This problem cannot be detected in laboratory tests using resistive loads and as a consequence the first deployment of the Scripps transmitter failed (Charles Cox, pers. comm.). This motivated the development of the inductive test load described above. One version of the commercial EM transmitter uses SCR switching but rather than using a zero-crossing detector the transmitter allows an 80 ms delay between switching polarities, creating a ternary waveform with a small off time (Mittet and Schaug-Pettersen 2008).

An alternative approach is to use a two-step rectification and switching process, first rectifying AC power using a diode bridge and then switching the 'DC' voltage using insulated gate bipolar transistors (IGBTs). Unlike SCRs, IGBTs can be turned off while conducting, although the peak values of the back EMF associated with switching the antenna inductance must be kept below the breakdown voltage of the diodes and IGBTs by including capacitors across the DC bus.

Although simple binary square waves at a fixed fundamental frequency were used by the Cambridge/Southampton transmitter (Sinha *et al.* 1990) and most of the early commercial CSEM surveys, more complicated waveforms are possible. Indeed, the early Scripps surveys used a ternary waveform that generated first and third harmonics of equal amplitude and minimized power at the higher frequencies (Constable and Cox 1996). Lu and Srnka (2005) described ternary waveforms designed to achieve a similar result with three or more harmonics spaced logarithmically in frequency. Mittet and Schaug-Pettersen (2008) described an optimization technique to create binary waveforms approximating a pre-determined frequency content. Myer *et al.* (2011) compared these and introduced yet another waveform having a broad frequency content.

Communication

Modern oceanographic and remotely operated vehicle (ROV) cables consist of outside armour/strength members protecting 3 power cables and one or more fibre optic lines. Although the

handling of fibre optic underwater terminations and slip rings (allowing continuous communication and power through a turning winch drum) is expensive, somewhat complicated and subject to failures, this approach is routine and standard for industry and most contractors use these types of cables, custom manufactured to handle the high voltages and currents needed for CSEM transmission. The use of fibre optic communication lines allows high-data rate communication, which is completely isolated from the power systems.

Many academic transmitter systems are designed to work on an older wireline standard of 17 mm diameter armoured cable with characteristics similar to RG8 coaxial cable. This cable is commonly available on many oceanographic vessels and a standard option for the UNOLS fleet. The terminations and slip rings for this cable are inexpensive, simple and reliable. In this case the usual approach is to overlay audio frequency-shift keyed (FSK) telemetry over the power transmission, using filters to separate the communication signals both on the ship and in the transmitter.

Navigation and ancillary systems

Probably the biggest limitation on CSEM data interpretation is source-receiver navigation. The cross-sectional area of the deep-tow cable (17 square metres per kilometre of cable in the case of the UNOLS coax, more in the case of higher power cables used for commercial CSEM) limits tow speeds to about 1.5 knots (0.8 m/s) in order to avoid the transmitter package 'kiting' behind the vessel. Even at these slow speeds, layback angles of 30–45 degrees are often encountered, placing the transmitter behind the vessel at a distance equal to as much as the water depth. As with receiver navigation, acoustic systems provide the only solution for determining the transmitter positions, since cumulative error in inertial navigations systems quickly become too large without periodic correction.

Navigation for the first Scripps transmitter was accomplished by attaching a free-running 12 kHz acoustic pinger to the tow cable above the transformer unit. The direct arrival and the reflection off the sea-floor were monitored at the ship in order to keep the transmitter package about 10 m above the sea-floor while the antenna dragged in contact with the sea-floor. Deployed cable and water depth were used to triangulate the position of the package, which was assumed to be behind the vessel along the ship's track. This sounds (and is) awfully crude but it is worth remembering that prior to GPS navigation the actual ship's position was not known to better than 500 m or so. Since source-receiver distances for the lithospheric soundings carried out this way were as large as 95 km (e.g., Constable and Cox 1996), this inaccuracy was tolerable. Similar systems are used to navigate towed source-receiver systems described below, where the source-receiver spacing is fixed by a cable array.

The simplest modern approach to determining the transmitter location is to mount a super short-baseline (SSBL) or ultra-short baseline (USBL) acoustic transponder on the transmitter package and antenna and use a ranging system mounted on the vessel. As we mention above, ideally one might expect range errors of no worse than 13 m given the specifications of these systems but this is likely optimistic and errors of up to 50 m have been anecdotally reported for CSEM transmitter positions. Because of the depth limitations of SSBL acoustics and the need to operate on various research vessels lacking permanently installed SSBL systems, academic groups have tended to use LBL navigation systems. The Southampton DASI was originally navigated using an installed array of LBL transponders moored about 200 m above the sea-floor. The need to be in range of the transponder array limited the area over which a survey could be carried out. Because the ranging system was installed on the vessel, a relay transponder was mounted on the transmitter, which complicated the geometry and reduced accuracy and reliability.

The Scripps group has attempted to overcome these limitations in LBL navigation by mounting the ranging instrument on the transmitter (rather than the vessel) and towing two transponders with GPS navigation systems on paravanes behind the vessel (Key and Constable, in preparation). This seems to work well and the transmitter can supplement the geometry by ranging directly on any of the sea-floor receivers, although the curvature of the raypaths limits the distance over which one can range to sea-floor transponders and the reply ping puts a noise spike in the EM data.

It should be noted that in order to recover the orientation of the transmitter antenna (the dip and cross-line set), one needs the position of both the head and tail of the instrument. The antenna dip can be recovered using a recording depth gauge on the tail but the cross-line set still needs acoustic positioning. In shallow water the layback angle of the antenna tail may exceed the capabilities of the SSBL equipment and so contractors are beginning to use SSBL systems that range directly from the head to the tail. Of course, one still needs the position of the head and now also the orientation.

Acoustic navigation is invariably supplemented by other sensors. Acoustic altimeters operating at high frequency and mounted on the transmitter can provide accurate (to a few centimetres) ranges to the sea-floor when the transmitter is within about 200 m of the sea-bottom. Precision pressure

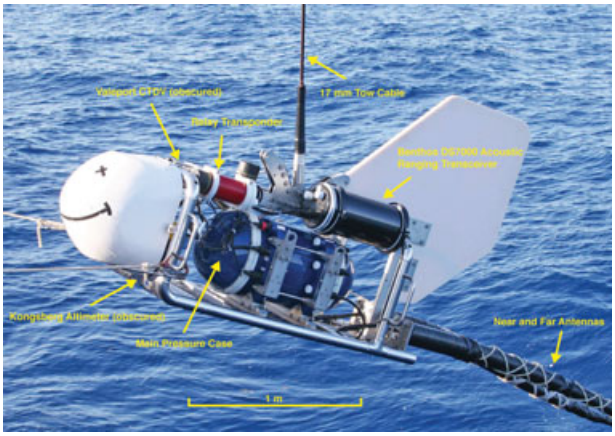

Figure 13 Scripps SUESI-500 EM transmitter being recovered.

gauges provide depths for the transmitter and antenna accurate to better than one metre. Inertial navigation systems can also be mounted on the transmitter to improve the navigation model. Sound velocity measurements made by sensors on the transmitter will increase the accuracy of the acoustic travel-time to range conversion, although these would normally be supplemented by daily expendable bathy-thermograph (XBT) casts from the vessel to infer near-surface velocities.

6.5 Scripps transmitter systems

The current Scripps transmitter system, called SUESI (Scripps Undersea Electromagnetic Source Instrument, shown in an annotated photograph in Fig. 13) is rated to a maximum output of 500 A (SUESI-500) and has been in use since 2006. A prototype rated at a maximum output current of 200 A (SUESI-200) was used in an experiment on the East Pacific Rise in February 2004 and on Hydrate Ridge in August 2004 (Weitemeyer *et al.* 2006).

The transmitters have a maximum depth rating of 6 km and are designed to operate using the standard UNOLS 0.680 inch (17.27 mm) coaxial wireline cable, which has a maximum working load of 10 000 lbs (44 kN), a loop resistance of 6.7 Ω/km, a capacitance of 0.108 μF/km and a maximum voltage rating of 3000 Vdc (2100 Vrms). The electromechanical termination of this cable can be carried out in about 3 hours and achieves the full working strength of the cable. We have achieved the maximum output current for the SUESI-500 on a neutrally buoyant 200 m antenna consisting in a 2 cm diameter aluminium conductor jacketed by a 5.6 cm diameter thermoplastic elastomer jacket but more typically use 300 A on a 250 m antenna for a maximum dipole moment of 95 kAm (square wave fundamental) or 200 A on a 50 m antenna for shallower hydrate mapping. The device is housed in a single 40 cm diameter pressure case that is air cooled internally and during a 300 A 100% duty cycle transmission operates at about 25° C above water temperature.

The original Scripps transmitter (Constable and Cox 1996; Fig. 14) used a simple Variac to provide ship's 60 Hz single phase power to a conventional 60 Hz step-up transformer. The bottom-side package used another conventional transformer for the step-down to high current and an SCR bridge for rectification and switching. For the SUESI transmitters the bottom-side transformers were made smaller by using a tow cable power frequency of 400 Hz (Fig. 15). Although most residential and commercial power systems work at 50 or 60 Hz, the higher frequency is used extensively in aerospace for exactly the same reasons that drive sea-floor instrumentation (smaller, lighter parts) and so components and design programs are available for this operating frequency. A toroidal transformer can also be employed to reduce size. This approach requires a topside system that can supply 400 Hz power from the ship's 50/60 Hz three-phase power. The SUESI systems use commercial 30 kVA switching power supplies/amplifiers designed to test large motors and machinery. This has the advantage that clean and stable power can be supplied to the tow cable and bottom package. Although these systems can supply 50, 60 and 400 Hz power using control from internal oscillators, we use a 400 Hz output from a GPS clock to generate a 400 Hz sine wave of variable amplitude to control the power supply. This means that the bottom-side package has GPS time provided by the power signal, which is used to clock all critical functions of the transmitter and particularly waveform switching. In this way the absolute phase for the transmitter signal is maintained throughout operation, leaving only the clock drift in the receiver instruments as a source of phase error. A transformer on the output of the topside power supply produces 2000 Vrms and 15 A on the tow cable.

As noted above, the power budget is determined by antenna resistance and tow cable voltage. The following analysis describes the design goal of 500 A on a 200 m antenna, achieved using a 4000 m tow cable. (In practice longer antennas and tow cables, along with a desire to operate with some headroom for cable voltage and transformer temperatures, restricts normal use to 300–400 A.) The 200 m antenna with a 2 cm aluminium conductor has a cable resistance of 0.033 Ω. Typically the electrode length is 10–20% of the antenna length, made from 3/4" soft copper tubing attached to the main antenna with standard compression pipe fittings. Minimizing electrode resistance is a matter of maximizing length but at some point resistive losses along the electrode become

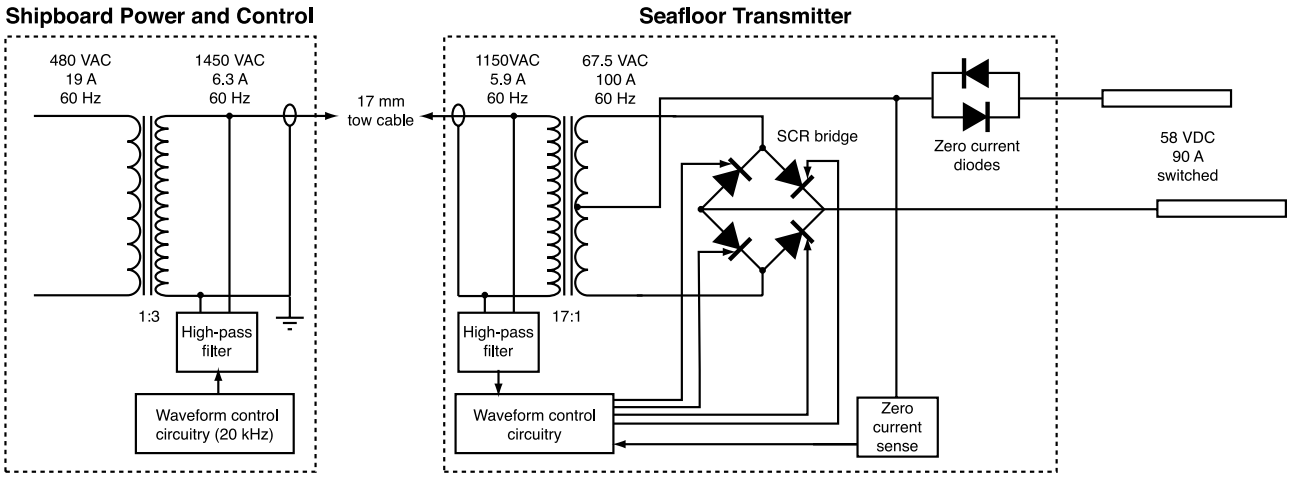

Figure 14 The original Scripps EM transmitter (Constable and Cox 1996), which used a simple Variac to provide 0–480 VAC from the ship's power to a step-up transformer. Waveform switching was provided by a simple 20 kHz control signal overlain on the 60 Hz power and was used to control an SCR bridge.

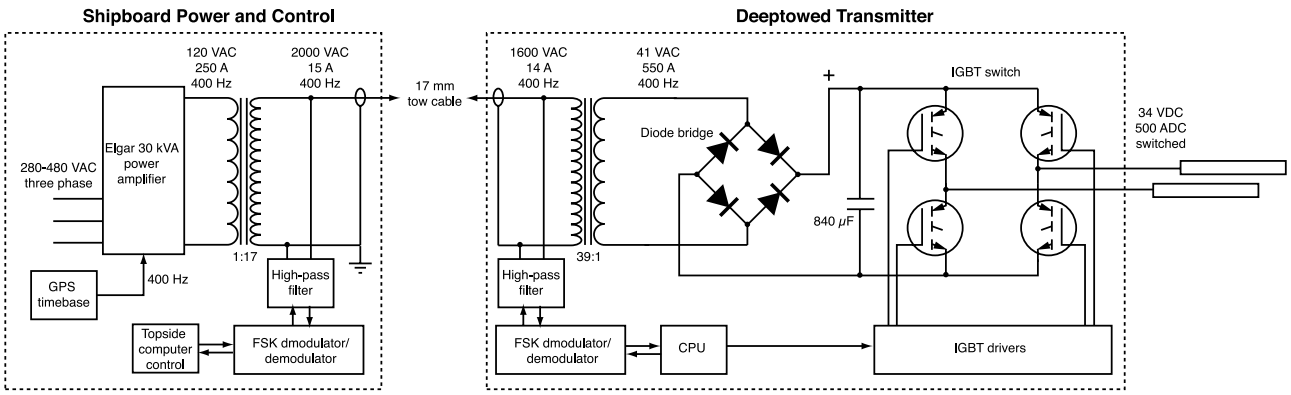

Figure 15 The current Scripps EM transmitter, which provides 400 Hz power to the tow cable. Waveform switching is done under computer control in the underwater unit, under instruction from a FSK serial link overlain on the power.

significant. The actual diameter of the 3/4" tubing is 2.22 cm, so a 20 m length has a grounding resistance in seawater of 0.017 Ω. Thus the total resistance of a 200 m long SUESI-500 antenna and two electrodes is 0.067 Ω, providing the maximum output current of 500 A with 34 V across the antenna. The inductance of this antenna is about 400 μH, which is balanced by 840 μF of capacitance across the transmitter output.

For the SUESI an SCR bridge was replaced with a separate diode bridge and IGBT switches controlled by an onboard computer, which uses a downloaded and stored waveform. If we add to the 34 V antenna voltage the drops across the semiconductors used in the rectification (1.4 V), drops across the switching circuits (about 2 V) and the rectification factor (1.11, the ratio of the RMS voltage to the average voltage), we obtain the voltage needed on the secondary side of the bottom-side transformer (41 V). However, before a bottom-side turns ratio can be computed one needs to take into account the voltage drop due to tow cable resistance. The return resistance for 4 km of UNOLS coaxial cable is 27 Ω and so the cable drop is about 400 V. We also lose about an amp to capacitive losses in the cable. This leads to two simultaneous equations in the two unknowns by expressing the turns ratio TR in terms of both the current and voltage ratios:

$$TR = \frac{I_{antenna}}{I_{cable}} \tag{16}$$

$$TR = \frac{V_{topside} - I_{cable} R_{cable}}{V_{antenna}}. \tag{17}$$

For the SUESI-500 example, these would be satisfied with a turns ratio of about 39.

For testing the SUESI-200 transmitter, we built a dummy load from 78 turns of #16 wire on a 19 cm diameter coil 28 cm long, for a resistance of 0.62 Ω and an inductance of 595 μH. This solenoid fits conveniently into a 20 litre plastic container and could be placed in a sink and water run through it for cooling. For the SUESI-500 transmitter, we used 3 parallel strands of #8 wire of length 85 m wound on a diameter of 35.5 cm, for a resistance of 0.06 Ω and inductance of 550 μH. Total height was 1.2 m and again this could be immersed in (a larger) plastic container of water for cooling.

Figure 16 shows a measurement of the output of the SUESI-500 operating at ±300 A, showing the extent of the residual ripple from the rectified 400 Hz and the switching transients associated with the bus capacitance. This waveform represents another attempt to broaden the frequency content of the CSEM signals and has nearly two decades of useful harmonics (Myer *et al.* 2011).

The overlay of communication on the 2000 VAC power (without fibre optics) is somewhat challenging. The original Scripps transmitter had a very limited one-way communication link in which either a 27 or 35 kHz control signal determined the polarity of waveform switching (no control signal determined an off state). The SUESI transmitters use an audio frequency-shift keyed (FSK) telemetry operating at 65.79/70.42 kHz on the uplink (transmitter to ship) and 121.9/128.2 kHz on the downlink (ship to transmitter). At these frequencies we were able to obtain reliable 9600 baud communication on tow cables up to 10 km long, allowing navigation and operational information to be monitored in real time. Peripheral sensors include a Valeport combination sound velocity and CTD probe, Kongsberg-Simrad 1007 series altimeter, pitch/roll/heading sensor and Benthos DS7000 intelligent acoustic transponder (7–16 kHz). Internal sensors include RMS output current and voltage, RMS cable voltage, main transformer temperature, diode temperatures and IGBT temperatures, which along with peripheral data are telemetered every 6 seconds to the vessel.

Periodically the entire waveform is digitized at sample rates up to 3600 Hz, buffered and then sent up the cable over a period of a minute or so. Since the phase is completely stable as a result of the GPS timing and the RMS output current is continuously monitored, this provides a complete description of the output waveform. Because waveform control and peripheral data handling are carried out by an onboard computer, downlink communication is limited to setting up the waveform characteristics, starting and stopping transmission and setting some navigation parameters.

7 TOWED SOURCE-RECEIVER SYSTEMS

To obtain deep soundings using large source-receiver offsets there is no alternative to the deployed sea-floor receiver, both from logistical and signal-to-noise ratio considerations. However, if one is interested in a shallow structure, typically associated with studies of sea-floor gas hydrates or hydrogeology, then deployed receivers become very difficult to place and navigate to the required accuracy and are also logistically inefficient ways to collect data. It is possible to package commercial equipment for submarine use, especially for operation in shallow water. Müller *et al.* (2010; 2012) installed a GEM-3 frequency-domain EM system in an oil-filled case mounted on a bottom-dragged sled for hydrogeological studies. Goldman *et al.* (2011) deployed Geonics EM-67 time-domain vertical component coils in plastic cases in 10 m water and floated a 100 m, 20 A, transmitter dipole on the surface.

Short source-receiver spacing can be achieved by towing or dragging receivers at fixed offsets behind the transmitter. This approach also offers the possibility of real-time data, although one needs to be careful to avoid cross-talk if source and receivers are coupled using a galvanic communication cable. The Geological Survey of Canada developed such a system that is dragged continuously on the sea-floor and uses a horizontal magnetic coil transmitter along with three horizontal magnetic receivers spaced at 4, 13 and 40 m behind it (Cheesman, Law and St. Louis 1993). A second such system was built by Woods Hole Oceanographic Institution (Evans 2007) for the study of groundwater and gas hydrate. Designed to operate on the 17 mm UNOLS cable, the Woods Hole transmitter uses a 9600 baud FSK telemetry system similar to the one described above and uses a 500 W DC power transmission system to provide ±24 V at the sea-floor, which is then switched under computer control at multiple frequencies, typically between 200 Hz and 200 kHz. Rather than log continuous time series, the independently (battery) powered receivers filter the signal at three frequencies (chosen according to offset) and determine the amplitude and phase averaged over 20 s recording windows. These data are then telemetered to the transmitter unit over a fibre optic cable (used to avoid galvanic cross-talk and coupling between transmitter and receiver) for transmission to the vessel in real time over the FSK link. Data can be collected during towing and at typical speeds of 1–2 knots this produces data at 10–20 m spacing. Published work relied on navigation obtained from wire length and water depth but SSBL acoustic navigation was reportedly used on more recent surveys. The system can be calibrated by making

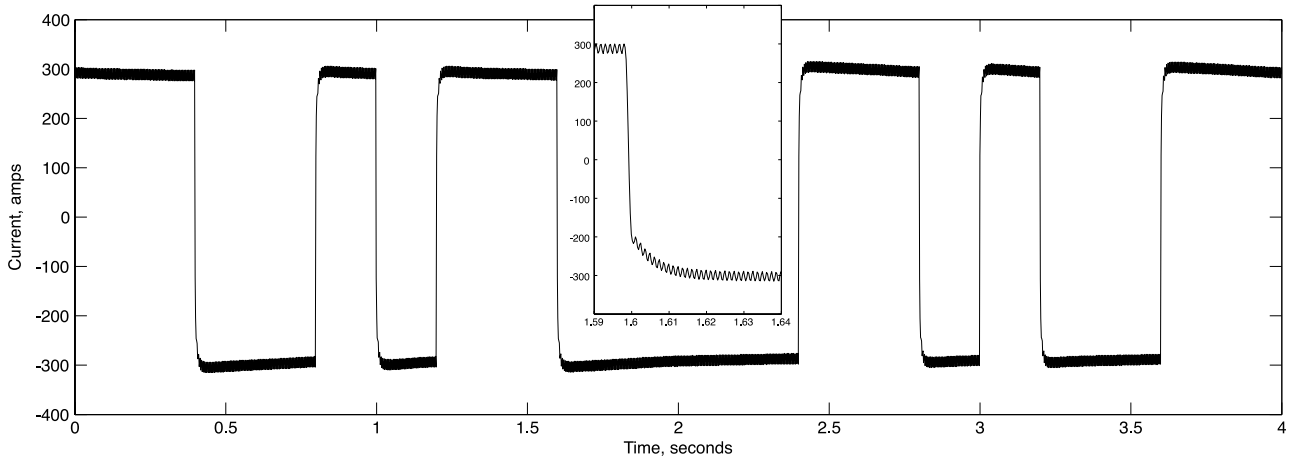

Figure 16 Output of SUESI-500 operating in seawater at 300 amps, sampled at 600 Hz. This waveform has nearly two decades of useful frequency content (Myer *et al.* 2011). The 'fuzz' is the aliased signature of the 800 Hz ripple remaining after rectification of the 400 Hz power and smoothing by the antenna inductance and capacitance across the DC bus. The inset shows a 50 ms segment during a transition, sampled at 3.6 kHz.

measurements in mid-water and comparing them to the onboard CTD sensor.

An instrument that is otherwise similar but uses horizontal electric transmitters and receivers was built at the University of Toronto (Yuan and Edwards 2000) and has 2 receiver channels spaced 377 and 493 m from the transmitter. Schwalenberg *et al.* (2010) used the Toronto system to study sea-floor gas hydrates off New Zealand. A 126 m long transmitter dipole was towed behind a sea-floor depressor weight and broadcast a 10 A peak-to-peak square wave at a period of 3.4 s. The transmission current was sent directly down the coaxial tow cable. Navigation was accomplished using an acoustic transponder mounted on the depressor weight. Two 15 m long receiver dipoles using silver chloride electrodes were towed behind the transmitter at offsets between 172–705 m. The receivers were self-contained logging units in order to avoid cross-talk between the transmitter and receiver circuitry, sampling at about 1 kHz. The array was towed between measurement sites but stopped at each site to allow 15 minutes of stacked data to be collected. A survey off Canada was carried out using the same equipment and similar experimental parameters (Schwalenberg *et al.* 2005). The square wave transmission allows the data to be analysed either in the frequency domain (Schwalenberg *et al.* 2005) or as time-domain transients (Schwalenberg *et al.* 2010). Again, the system can be calibrated by making measurements in mid-water, although the motion of the system induces some noise. Schwalenberg's group has recently commissioned a new system having 4 receivers and a depressor weight instrumented with an acoustic transponder, CTD sensor and data communication with the receivers (Schwalenberg and Engels 2011).

Dragging equipment in contact with the sea-floor has the advantage of maximizing coupling and simplifying navigation and is almost the only way that very high-frequency, very short offset, data can be collected. However, this limits its operation to sedimented areas with no infrastructure and both Schwalenberg and Evans have had receivers torn off their equipment (although recovering hundreds of metres of cable from the seafloor by dragging hooks is usually successful). Another approach is to tow receivers as neutrally buoyant packages behind a deep-towed transmitter. Weitemeyer and Constable (2010) described data from a three-axis electric field receiver that was towed 300 m behind a 50 m/200 A transmitter during studies to map gas hydrate in the Gulf of Mexico. Like the Schwalenberg *et al.* (2010) system, the receivers relied on autonomous recording but also included depth, pitch, roll and heading sensors for navigation. Frequencies between 0.5–33.5 Hz were transmitted using the broad-spectrum frequency-domain waveform of Myer *et al.* (2011), providing some depth discrimination in spite of the single source-receiver offset. By towing the array within 60 m of the sea-floor reasonable coupling was achieved. High-quality data can be collected during normal transmitter tow speeds of 1–2 knots since streaming potentials, thought to be a problem for electric field systems (e.g., Evans 2007), are in practice not a significant source of noise. The largest noise in towed systems appears to be from lateral motion of antenna cables in the Earth's magnetic field and so the instrument

described by Weitemeyer and Constable (2010) uses short, rigid antennas.

Although technically not an inductive CSEM system, the DC resistivity system of Goto *et al.* (2008) is worth including here, since it operates in a similar way to the equipment described above and for the same purpose of mapping sea-floor gas hydrate in full ocean depths. It is based around JAMSTEC's deep-tow system that is designed to collect images and samples from within about 5 m of the sea-floor. Goto *et al.* (2008) equipped the deep-tow with a 160 m long DC resistivity array made neutrally buoyant using glass oceanographic flotation spheres. In a reversal of the approach taken by other groups, the 20 m receiver dipole is towed immediately behind the deep-tow and the transmitter electrodes are distributed between 56–157 m behind the instrument package. Rather than mount the silver chloride electrodes on the array, hoses form salt bridges to the measurement points. The system is navigated using SSBL transponders on the antenna tail and deep-tow and an acoustic altimeter on the deep-tow. The output waveform is a 4-second sinusoid with a 44 A peak-to-peak amplitude, switched every cycle between the seven transmitter electrodes (the far electrode is common). The system is calibrated in the usual way using measurements in mid-water and compared to the deep-tow's CTD sensor. The equipment was tested successfully in the Japan Sea.

Because of the logistical cost of deploying sea-floor instruments for hydrocarbon surveys, industry is trying to extend the towed receiver concept to large source-receiver offsets. Ziolkowski *et al.* (2010) described a bottom-dragged electric field system in which a 400 m/700 A transmitter antenna and a separate cable containing thirty 200 m receiver dipoles are towed behind two ships in order to obtain data at source-receiver offsets up to 7 km. Again, the vessels had to be stopped to make the measurements. It is not reported how long the measurements took but a single time-domain waveform at long offsets was 13.5 minutes long. Mattsson *et al.* (2010) reported the use of a near-surface towed version of this equipment with source-receiver offsets of up to 2.5 km. Both time-domain and frequency-domain transmissions were made but analysis seems to be in the frequency domain.

8 SUMMARY AND CONCLUSIONS

The development of marine EM equipment remains an active area of research and development for both industry and academia but these two sectors are driven by different considerations. Academia needs to minimize the cost of equipment and acquisition (because there is never enough research funding) and maximize flexibility, so that a variety of research vessels can be used to collect data in ways that are customized to meet a variety of research goals. Industry needs to commoditize the data, producing a reliable standard product that can be collected without extensive training of personnel. Of course, industry would also like to minimize acquisition costs but if the data have value to exploration and production then the market is likely to pay what it takes to collect them. Industry is certainly able to put considerable resources into equipment development and construction. It is therefore likely that industrial and academic marine EM equipment, which is currently very similar, will diverge, although the underlying principles will remain the same.

ACKNOWLEDGEMENTS

Thanks go to Charles (Chip) Cox first and foremost for introducing the author to the field of marine EM and making his knowledge and instrumentation available for future use and development. This generosity has had a truly significant impact on both the commercial and academic marine EM communities. Many thanks are also due to the numerous engineers and technicians who have helped design, develop, build and use the equipment described in this chapter, particularly Tom Deaton, Jacques Lemire and John Souders. Funding for the work presented here has been broad-based, mostly supported by the Scripps Sea-floor Electromagnetic Methods Consortium (http://marineemlab.ucsd.edu/semc.html) with special thanks to ExxonMobil, AGO and BHP Billiton. Critique by Katrin Schwalenberg and anonymous reviewers led to significant improvements in the manuscript.

REFERENCES

Becker K., VonHerzen R.P., Francis T.J.G., Anderson R.N., Honnorez J. and Adamson A.C. *et al.* 1982. *In situ* electrical resistivity and bulk porosity of the oceanic crust Costa Rica Rift. *Nature* **300**, 594–598.

Brown T.F. and Cox C.S. 1973. Design of light, cylindrical pressure cases. *Engineering Journal* **2**, 35–37.

Cheesman S.J., Law L.K. and St. Louis B. 1993. A porosity mapping survey in Hecate Straight using a seafloor electro-magnetic profiling system. *Marine Geology* **110**, 245–256.

Constable S.C. 1990. Marine electromagnetic induction studies. *Surveys in Geophysics* **11**, 303–327.

Constable S. and Cox C.S. 1996. Marine controlled source electromagnetic sounding 2. The PEGASUS experiment. *Journal of Geophysical Research* **101**, 5519–5530.

Constable C.G. and Constable S.C. 2004. Satellite magnetic field measurements: Applications in studying the deep Earth. In: *The State of the Planet: Frontiers and Challenges in Geophysics, Geophysical*

Monograph 150, (eds R.S.J. Sparks and C.T. Hawkesworth), pp. 147–159. American Geophysical Union.

Constable S. and Heinson G. 2004. Hawaiian hot-spot swell structure from seafloor MT sounding. *Tectonophysics* **389**, 111–124.

Constable S., Heinson G., Anderson G. and White A. 1997. Seafloor electromagnetic measurements above Axial Seamount, Juan de Fuca Ridge. *Journal of Geomagnetism and Geoelectricity* **49**, 1327–1342.

Constable S., Key K. and Lewis L. 2009. Mapping offshore sedimentary structure using electromagnetic methods and terrain effects in marine magnetotelluric data. *Geophysical Journal International* **176**, 431–442.

Constable S., Orange A., Hoversten G.M. and Morrison H.F. 1998. Marine magnetotellurics for petroleum exploration Part 1. A seafloor instrument system. *Geophysics* **63**, 816–825.

Constable S. and Srnka L.J. 2007. An introduction to marine controlled source electromagnetic methods for hydrocarbon exploration. *Geophysics* **72**, WA3–WA12.

Constable S. and Weiss C.J. 2005. Mapping thin resistors (and hydrocarbons) with marine EM methods: Insights from 1D modeling. *Geophysics* **71**, G43–G51.

Corwin R.F. 1973. *Offshore Application of Self-potential Prospecting*. PhD thesis, University of California, Berkeley (available as Scripps Institution of Oceanography Library, Paper 22, http://repositories.cdlib.org/sio/lib/22).

Cox C.S. 1980. Electromagnetic induction in the oceans and inferences on the constitution of the earth. *Geophysical Surveys* **4**, 137-156.

Cox C.S., Constable S.C., Chave A.D. and Webb S.C. 1986. Controlled source electromagnetic sounding of the oceanic lithosphere. *Nature* **320**, 52–54.

Cox C.S., Deaton T.K. and Pistek P. 1981. *An active source EM method for the seafloor*. Scripps Institution of Oceanography Technical Report, http://escholarship.org/uc/item/7dr96489, accessed 25 May 2010.

Cox C.S., Filloux J.H. and Larsen J.C. 1971. Electromagnetic studies of ocean currents and electrical conductivity below the ocean floor. In: *The Sea*, Vol. 4 Part I, (ed. A.E. Maxwell), pp. 637–693. Wiley–Interscience, New York.

Crona L., Fristedt T., Lundberg P. and Sigray P. 2001. Field tests of a new type of graphite-fiber electrode for measuring motionally induced voltages. *Journal of Atmospheric and Oceanic Technology* **18**, 92–99.

Ellingsrud S., Eidesmo T., Johansen S., Sinha M.C., MacGregor L.M. and Constable S. 2002. Remote sensing of hydrocarbon layers by seabed logging (SBL): Results from a cruise offshore Angola. *The Leading Edge* **21**, 972–982.

Evans R.L. 2007. Using CSEM techniques to map the shallow section of seafloor: From the coastline to the edges of the continental slope. *Geophysics* **72**, WA105–WA116.

Evans R.L., Constable S.C., Sinha M.C. and Cox C.S. 1991. Upper crustal resistivity structure of! the East Pacific Rise near 13°N. *Geophysical Research Letters* **18**, 1917–1920.

Evans R.L., Tarits P., Chave A.D., White A., Heinson G., Filloux J.H. *et al.* 1999. Asymmetric electrical structure in the mantle beneath the East Pacific rise at 17 degrees S. *Science* **286**, 752–756.

Filloux J.H. 1967. An ocean bottom, D component magnetometer. *Geophysics* **6**, 978–987.

Filloux J.H. 1974. Electric field recording on the sea floor with short span instruments. *Journal of Geomagnetism and Geoelectricity* **26**, 269–279.

Filloux J.H. 1987. Instrumentation and experimental methods for oceanic studies. In: *Geomagnetism*, (ed. J.A. Jacobs), pp. 143–248. Academic Press.

Goldman M., Levi E., Tezkan B. and Yogeshwar P. 2011. The 2D coastal effect on marine time domain electromagnetic measurements using broadside dBz/dt of an electrical transmitter dipole. *Geophysics* **76**, F101–F109.

Goto T., Kasaya T., Machiyama H., Takagi R., Matsumoto R., Okuda Y. *et al.* 2008. A marine deep-towed DC resistivity survey in a methane hydrate area, Japan Sea. *Exploration Geophysics* **39**, 52–59.

Heinson G., Constable S. and White A. 1996. Seafloor magnetotelluric sounding above Axial seamount. *Geophysical Research Letters* **23**, 2275–2278.

Heinson G., Constable S. and White A. 2000. Episodic melt transport at a mid-ocean ridge inferred from magne- totelluric sounding. *Geophysical Research Letters* **27**, 2317–2320.

Heinson G.S., White A., Law L.K., Hamano Y., Utada H., Yukutake J. *et al.* 1993. EMRIDGE: The electromagnetic investigation of the Juan de Fuca Ridge. *Marine Geophysical Researches* **5**, 77–100.

Hoehn G.L. and Warner B.N. 1983. Magnetotelluric measurements in the Gulf of Mexico at 20 m ocean depths. In: *CRC Handbook of Geophysical Exploration at Sea*, (ed. R.A. Geyer), pp. 397–416. CRC Press, Boca Raton.

Hoversten G.H., Constable S. and Morrison H.F. 2000. Marine magnetellurics for base salt mapping: Gulf of Mexico field-test at the Gemini structure. *Geophysics* **65**, 1476–1488.

Irons H.R. and Schwee L.J. 1972. Magnetic thin-film magnetometers for magnetic-field measurement. *IEEE Transactions on Magnetics*, **MAG-8**, 61–65.

Jegen M. and Edwards R.N. 1998. The electrical properties of a 2D conductive zone under the Juan de Fuca Ridge. *Geophysical Research Letters* **25**, 3647–3650.

Joseph E.J., Toh H., Fujimoto H., Iyengar R.V., Singh B.P., Utada H. and Segawa J. 2000. Seafloor electromagnetic induction studies in the Bay of Bengal. *Marine Geophysical Researches* **21**, 1–21.

Key K.W. 2003. *Application of Broadband Marine Magnetotelluric Exploration to a 3D Salt Structure and a Fast-Spreading Ridge*. PhD thesis, University of California San Diego.

Key K. 2009. 1D inversion of multicomponent, multifrequency marine CSEM data: Methodology and synthetic studies for resolving thin resistive layers. *Geophysics* **74**, F9–F20.

Key K.W., Constable S.C. and Weiss C.J. 2006. Mapping 3D salt using 2D marine MT: Case study from Gemini Prospect, Gulf of Mexico. *Geophysics* **71**, B17–B27.

Key K. and Lockwood A. 2010. Determining the orientation of marine CSEM receivers using orthogonal Procrustes rotation analysis. *Geophysics* **75**, F63–F70.

Knappe S., Gerginov V., Schwindt P.D.D., Shah V., Robinson H.G., Hollberg L. and Kitching J. 2005. Atomic vapor cells for chip-scale

atomic clocks with improved long-term frequency stability. *Optics Letters* **30**, 2351–2353.

Law L.K. 1978. An ocean bottom magnetometer: Design and first deployment near the Explorer Ridge (abstract). *Eos Transactions of the AGU* **59**, 235.

Law L.K. and Greenhouse J.P. 1981. Geomagnetic-variation sounding of the asthenosphere beneath the Juan-de Fuca Ridge. *Journal of Geophysical Research* **86**, 967–978.

Lu X. and Srnka L.J. 2005. Logarithmic spectrum transmitter waveform for controlled-source electromagnetic surveying. United States Patent 7539279.

Mattsson J., Lund L., Lima J., Engelmark F. and McKay A. 2010. Case study: A towed EM test at the Peon discovery in the North Sea. Contributed paper at EAGE Meeting, pages 1–5.

Mittet R., Aakervik O.M., Jensen H.R., Ellingsrud S. and Stovas A. 2007. On the orientation and absolute phase of marine CSEM receivers. *Geophysics* **72**, F145–F155.

Mittet R. and Schaug-Pettersen T. 2008. Shaping optimal transmitter waveforms for marine CSEM surveys. *Geo- physics* **73**, F97–F104.

Müller H., von Dobeneck T., Hilgenfeldt C., SanFilipo B., Rey D. and Rubio B. 2012. Mapping the magnetic susceptibility and electric conductivity of marine surficial sediments by benthic EM profiling. *Geophysics* **77**, E43–E56.

Müller H., von Dobeneck T., Nehmiz W. and Hamer K. 2011. Near-surface electromagnetic, rock magnetic, and geochemical fingerprinting of submarine freshwater seepage at Eckernforde Bay (SW Baltic Sea). *Geo-Marine Letters* **31**, 123–140.

Myer D., Constable S. and Key K. 2011. Broad-band waveforms and robust processing for marine CSEM surveys. *Geophysical Journal International* **184**, 689–698.

Myer D., Constable S. and Key K. 2012. Marine CSEM survey of the Scarborough gas field, Part 1: Experimental design and data uncertainty. *Geophysics* **77**, E281–E299.

Orange A., Key K. and Constable S. 2009. The feasibility of reservoir monitoring using time-lapse marine CSEM. *Geophysics* **74**, F21–F29.

Perkin R.G. and Walker E.R. 1972. Salinity calculations from in situ measurements. *Journal of Geophysical Research* **77**, 6618–6621.

Poehls K.A. and Von Herzen R.P. 1976. Electrical resistivity structure beneath the North-west Atlantic Ocean. *Geophysical Journal of the Royal Astronomical Society* **47**, 331–346.

Ripka P. 1992. Review of fluxgate sensors. *Sensors and Actuators A* **33**, 129–141.

Rosa E.B. 1908. The Self and Mutual Inductances of Linear Conductors. *Bulletin of the Bureau of Standards* **4**, 301.

Schwalenberg K. and Engels M. 2011. Marine controlled source electromagnetic methods for gas hydrate assessment: New instrumentation and first field applications. Contributed paper at *Proceedings of the 7th International Conference on Gas Hydrates,* Edinburgh, UK, July, pp. 17–21.

Schwalenberg K., Haeckel M., Poort J. and Jegen M. 2010. Evaluation of gas hydrate deposits in an active seep area using marine controlled source electromagnetics: Results from Opouawe Bank, Hikurangi Margin, New Zealand. *Marine Geology* **272**, 79–88.

Schwalenberg K., Willoughby E., Mir R. and Edwards R.N. 2005. Marine gas hydrate electromagnetic signatures in Cascadia and their correlation with seismic blank zones. *First Break* **23**, 57–63.

Segawa J. and Toh H. 1992. Detecting fluid circulation by electric-field variations at the Nankai Trough. *Earth and Planetary Science Letters* **109**, 469–476.

Sinha M.C., Navin D.A., MacGregor L.M., Constable S., Peirce C., White A. *et al.* 1996. Evidence for accumulated melt beneath the slow-spreading mid-Atlantic ridge. *Philosophical Transactions A Royal Society* **355**, 233–253.

Sinha M.C., Patel P.D., Unsworth M.J., Owen T.R.E. and MacCormack M.R.J. 1990. An active source EM sounding system for marine use. *Marine Geophysical Research* **12**, 59–68.

Spiess F.N. and Mudie J.D. 1970. Small-scale topographic and magnetic features. In: *The Sea*, Vol. 4 Part I (ed. A.E. Maxwell), pp. 637–693. Wiley–Interscience, New York.

Spiess F.N. and Tyce T.C. 1973. Marine Physical Laboratory Deep Tow Instrument System. Scripps Institution of Oceanography Reference 73–74, 37 pp.

Sunde E.D. 1949. *Earth Conduction Effects in Transmission Systems*. D. Van Nostrand, New York.

Toh H., Goto T. and Hamano Y. 1998. A new seafloor electromagnetic station with an Overhauser magnetometer, a magnetotelluric variograph and an acoustic telemetry modem. *Earth, Planets and Space* **50**, 895–903.

Tumanski S. 2007. Induction coil sensors – A review. *Measurement Science and Technology* **18**, R31–R46.

Webb S.C., Constable S.C., Cox C.S. and Deaton T.K. 1985. A seafloor electric field instrument. *Geomagnetism and Geoelectricity* **37**, 1115–1129.

Weitemeyer K.A. 2008. *Marine Electromagnetic Methods for Gas Hydrate Characterization*. PhD thesis, University of California, San Diego (available as Scripps Institution of Oceanography Technical Report, http://repositories.cdlib.org/sio/techreport/91.

Weitemeyer K. and Constable S. 2010. Mapping shallow geology and gas hydrate with marine CSEM surveys. *First Break* **28**, 97–102.

Weitemeyer K.A., Constable S.C., Key K.W. and Behrens J.P. 2006. First results from a marine controlled-source electromagnetic survey to detect gas hydrates offshore Oregon. *Geophysical Research Letters* **33**, L03304, doi:10.1029/2005GL024896.

Wheeler H.A. 1928. Simple inductance formulas for radio coils. *Proceedings of the Institute of Radio Engineering*, **16**, 1398–1400.

White A. 1979. A sea floor magnetometer for the continental shelf. *Marine Geophysical Researches* **4**, 105–114.

Worzewski T., Jegen M., Kopp H., Brasse H. and Castillo W.T. 2011. Magnetotelluric image of the fluid cycle in the Costa Rican subduction zone. *Nature Geoscience* **4**, 108–111.

Yuan J. and Edwards R.N. 2000. The assessment of marine gas hydrates through electrical remote sounding: Hydrate without a BSR? *Geophysical Research Letters* **27**, 2397–2400.

Ziolkowski A., Parr R., Wright D., Nockles V., Limond C., Morris E. and Linfoot J. 2010. Multi-transient electromagnetic repeatability experiment over the North Sea Harding field. *Geophysical Prospecting* **58**, 1159–1176.